# Neutron Star Physics
## -Fifty Years after the Discovery-

**Kei Iida (Kochi University)**

*Contents*

- *Introduction: Neutron stars and pulsars*
- *Neutron star matter*
- *Low-density neutron matter vs. trapped cold atoms*
- *Neutron superfluidity and vortices*
- *Nuclear pasta, liquid crystals, cuprates, and gyroids*
- *Low-mass neutron stars as giant atomic nucei*

# Discovery of pulsars and neutron star observations

In 1967, Hewish & Bell discovered a "pulsar" emitting periodic radio pulses, PSR B1919+21 (at that time, referred to as LGM "Little Green Men"-1.)

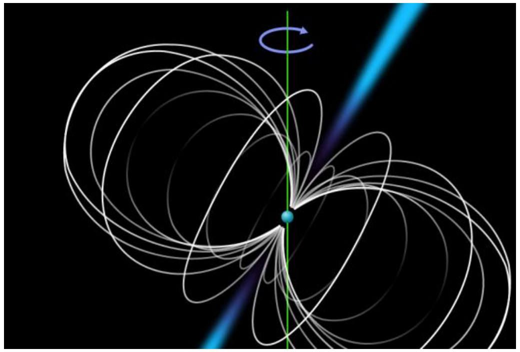

Imaginary drawing of a pulsar (gigantic "dynamo")

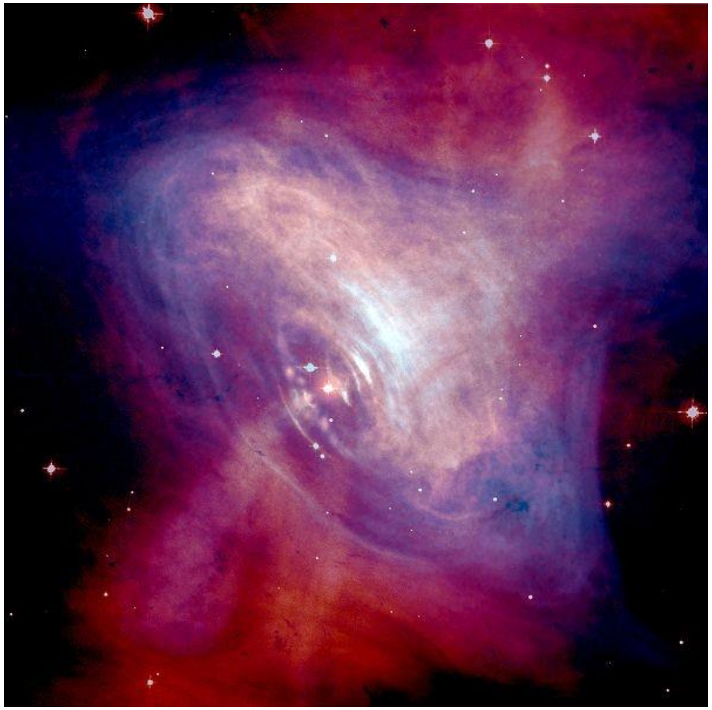

Crab Nebula (NASA/ESA)

1968: A pulsar discovered in the Crab Nebula.

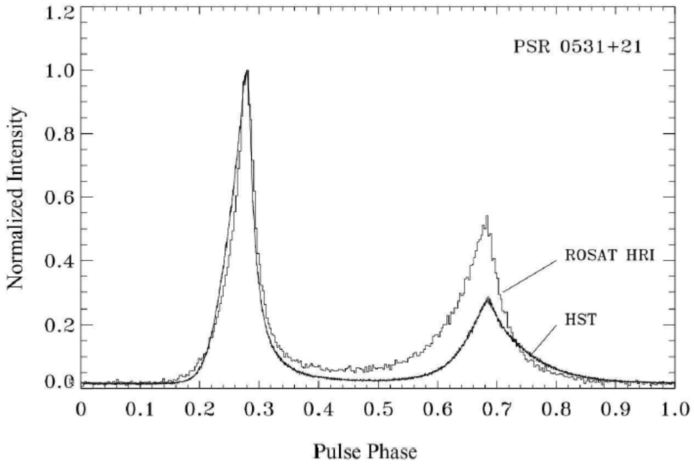


The very short (33 msec) period of the Crab pulsar helped to identify pulsars as neutron stars!

# Discovery of pulsars and neutron star observations (contd.)

In 1962, as a start of X-ray astronomy, Rossi, Giacconi et al. discovered an X-ray source (Sco X-1), which was eventually identified as a neutron star.

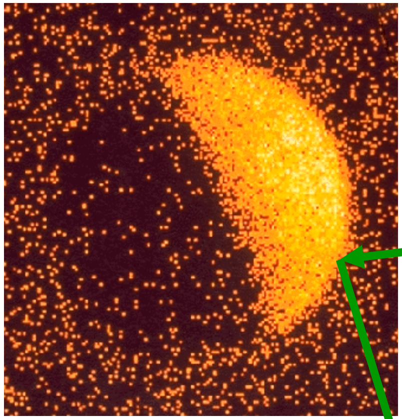

X-ray image of the Moon

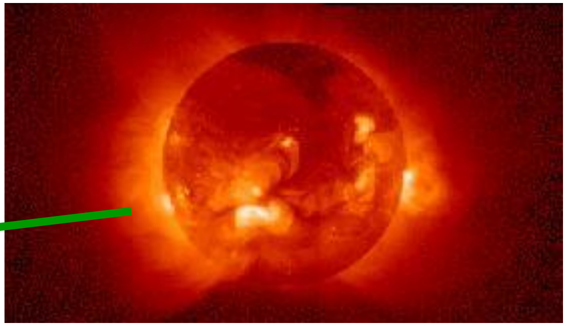

X-ray image of the Sun

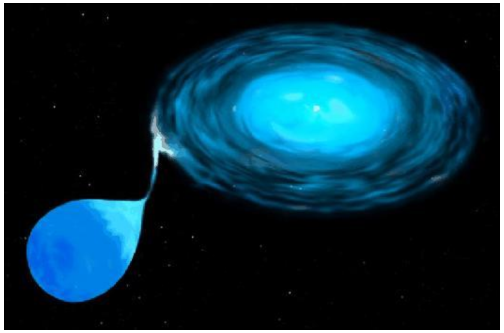

Imaginary drawing of Sco X-1

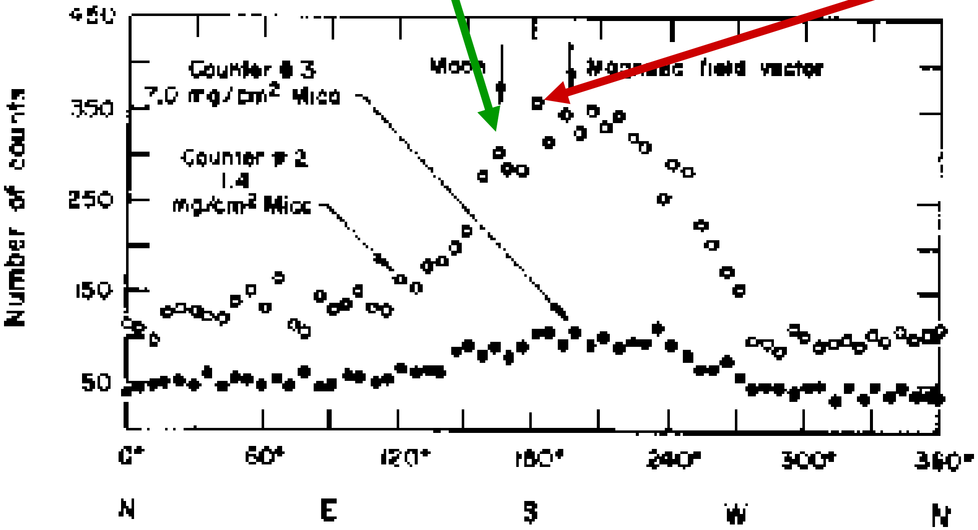


X-ray observation by a rocket

http://chandra.harvard.edu/xray_sources/sco/sco.html

# Discovery of pulsars and neutron star observations (contd.)

In 1997, a nearby neutron star (about 100 pc away) was discovered by an X-ray telescope ROSAT.

RX J1856.5-3754 (one of “Magnificent Seven”)
NASA/SAO/CXC/J.Drake et al.

Yet to be seen as a radio pulsar.

The X-ray emission: approx. blackbody spectrum & periodicity of about 7 sec.

Distance marginally measurable from the optical parallax.

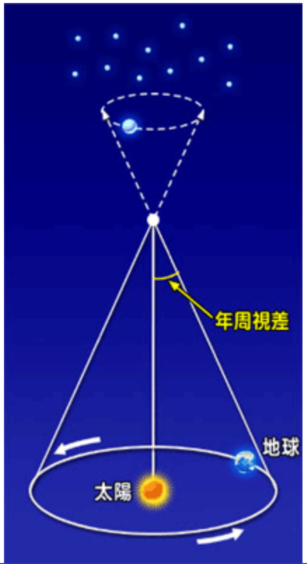

# Pulsars as precise clocks

In 1982, a “msec pulsar” (about 1.6 ms periodicity) was discovered.

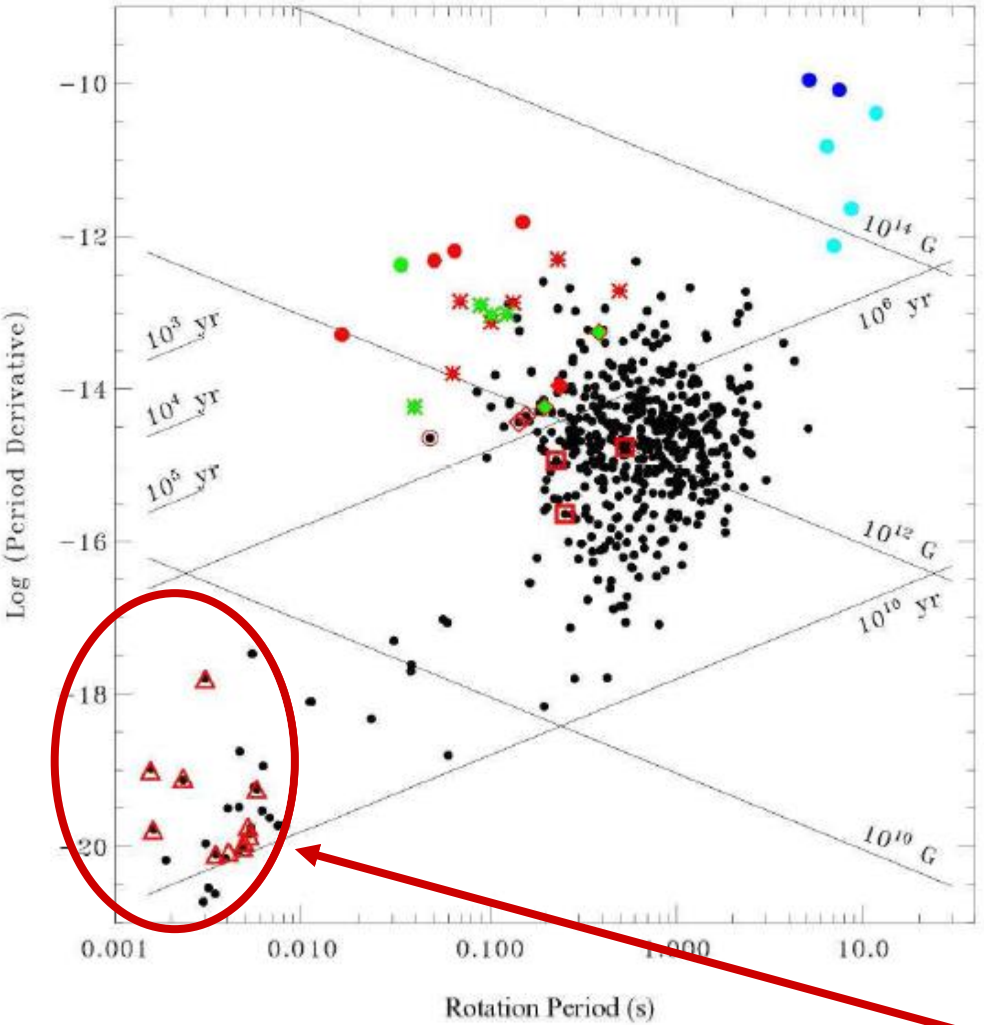


arXiv:astro-ph/0208356

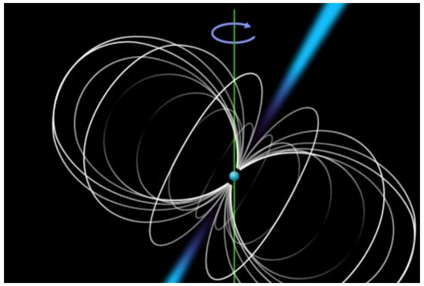

Evolved from a X-ray binary system

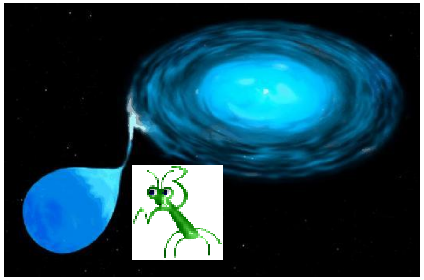

Stable rotation and sharp radio pulses of msec pulsars
→clocks that can be as stable as atomic clocks!

# Pulsars as precise clocks (contd.)

Pulse profiles of msec pulsars (MSPs)

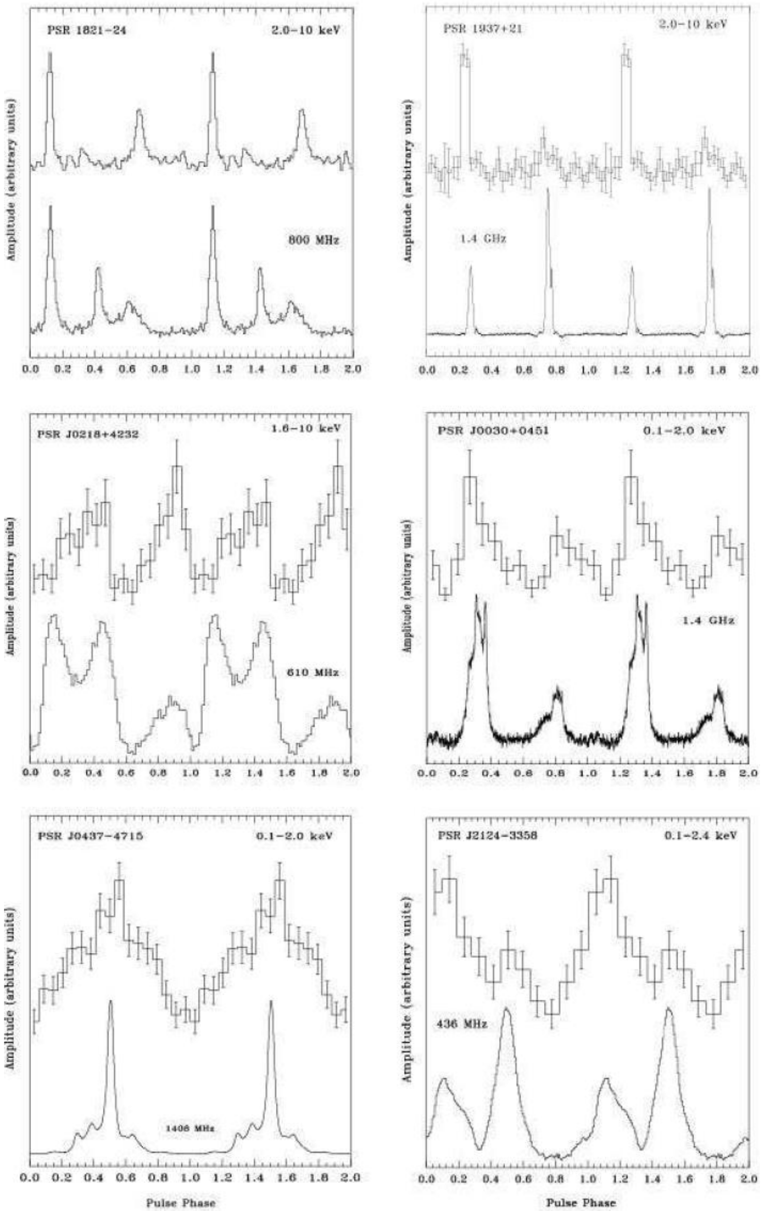


The nearest MSP:
PSR J0437-4715

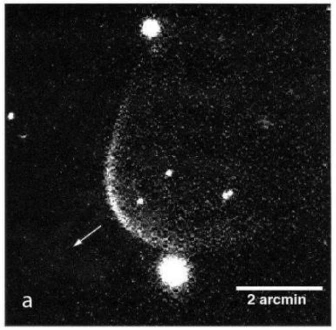


Planet-hosting MSP:
PSR B1257+12

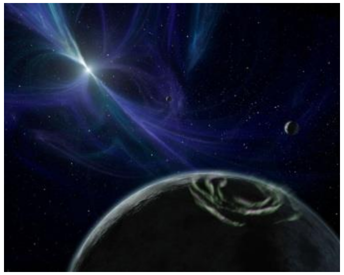

Imaginary drawing by NASA

19 MSPs in the globular cluster 47 Tuc!

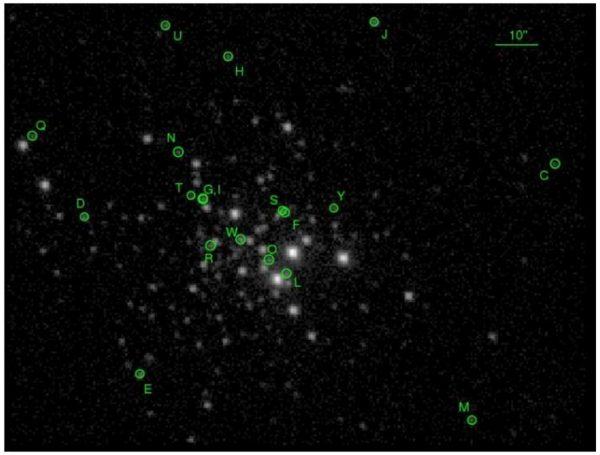


arXiv:astro-ph/0208356, NASA/CXC/CfA/S. Bogdanov

# Diagnosing the interstellar medium

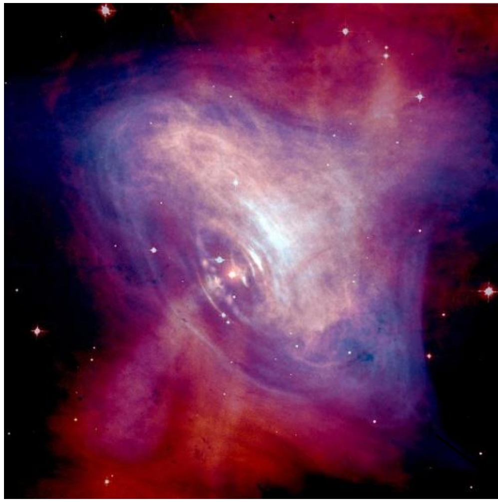

Pulsar (NASA/ESA)

How is the interstellar medium (ISM) ionized? How are stars born in the ISM?

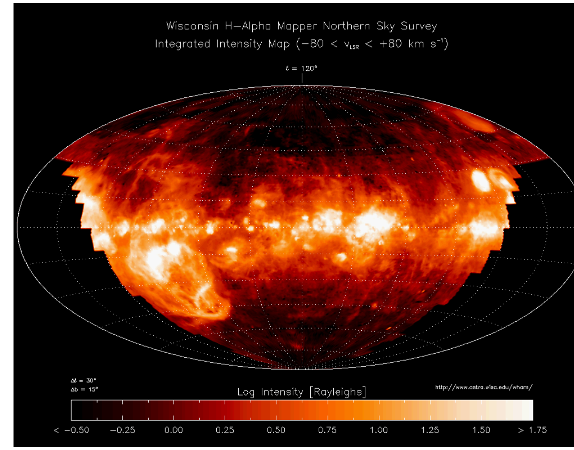


Distribution of ionized hydrogens

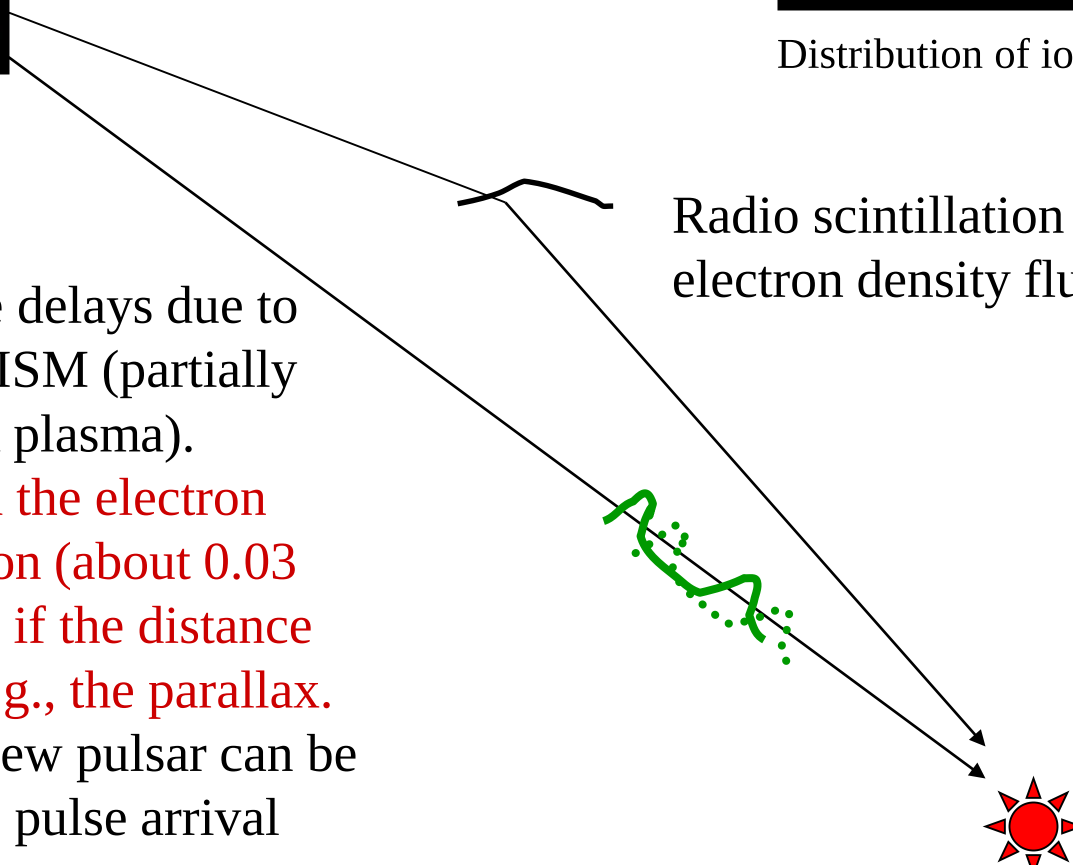

Radio scintillation due to electron density fluctuations

Pulse arrival time delays due to dispersion in the ISM (partially ionized hydrogen plasma).
→Information on the electron density distribution (about 0.03 $cm^{-3}$ on average ) if the distance is known from, e.g., the parallax.
→Distance to a new pulsar can be deduced from the pulse arrival time delay.

# Pulsar glitch

From young pulsars, glitches, sudden decrease in the pulse period, are frequently observed.

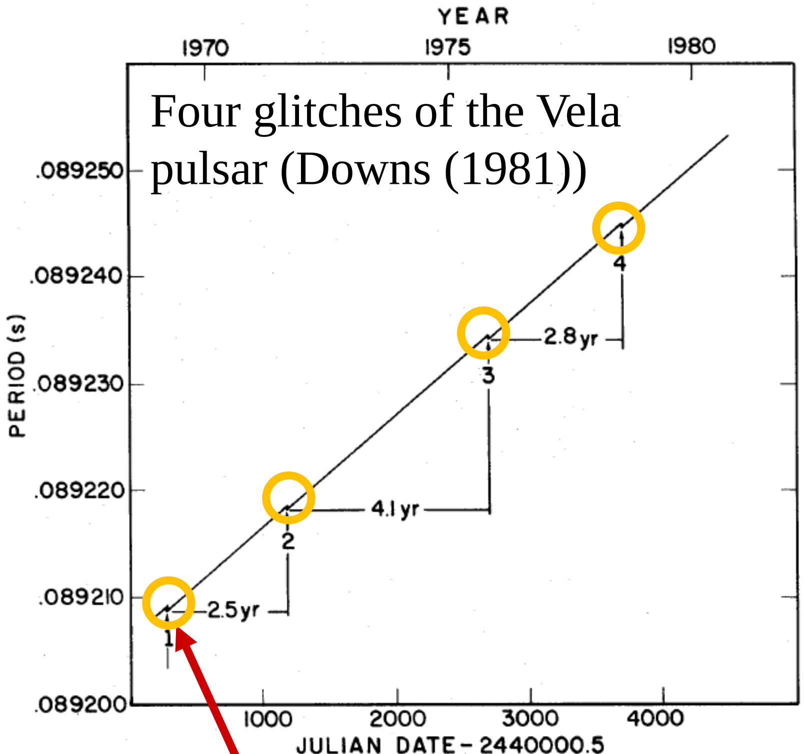


Four glitches of the Vela pulsar (Downs (1981))

Consistent with backreaction to disappearance of outwardly moving vortices, suggesting that superfluidity should occur in a neutron star!

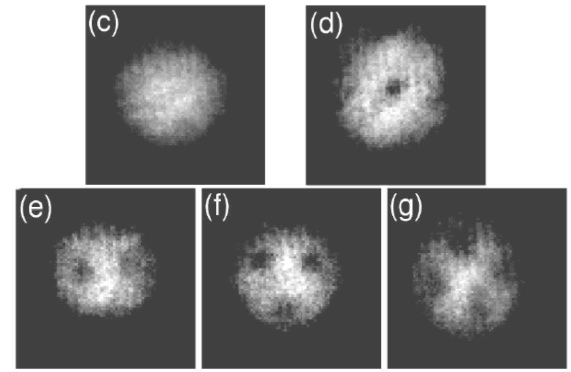


Vortices in rotating Bose condensate of Rb atoms (Madison et al.(2000))

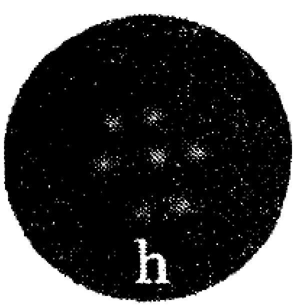


Vortices in rotating superfluid helium (Yarmchuk et al.(1979))

# Neutron star mass determination by Hulse & Taylor

A pulsar with a binary companion:
Observed orbital motion → mass measurement!

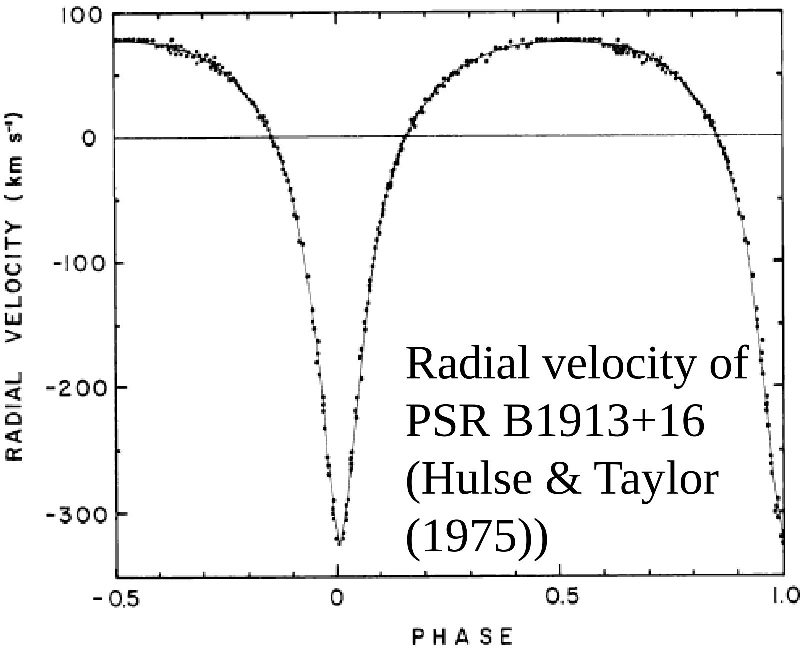


The companion of PSR B1913+16 is also a neutron star!

⇩

Post-Keplerian orbit!

⇩

General relativity allows accurate mass determination!

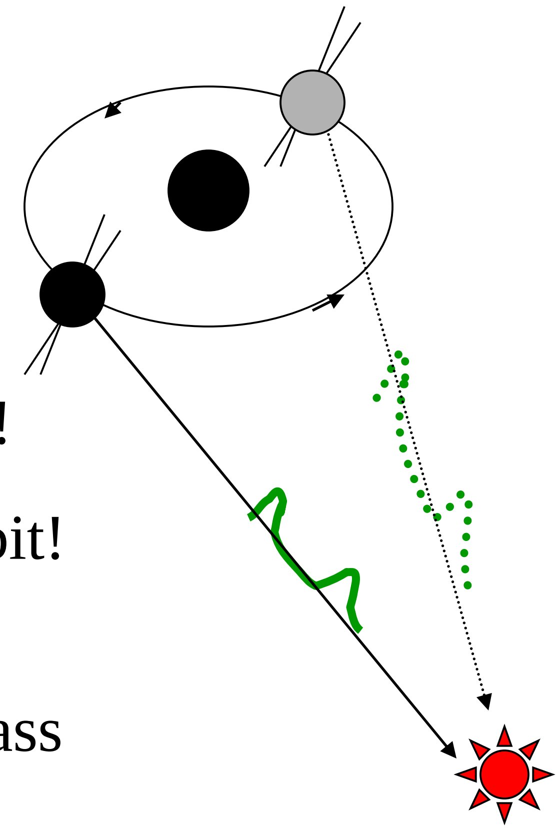

| *Neutron star–neutron star binaries* | | | | | |
|---|---|---|---|---|---|
| 1518+49 | $1.56^{+0.13}_{-0.44}$ | (*88*) | 1518+49 companion | $1.05^{+0.45}_{-0.11}$ | (*88*) |
| 1534+12 | $1.3332^{+0.0010}_{-0.0010}$ | (*88*) | 1534+12 companion | $1.3452^{+0.0010}_{-0.0010}$ | (*88*) |
| 1913+16 | $1.4408^{+0.0003}_{-0.0003}$ | (*88*) | 1913+16 companion | $1.3873^{+0.0003}_{-0.0003}$ | (*88*) |
| 2127+11C | $1.349^{+0.040}_{-0.040}$ | (*88*) | 2127+11C companion | $1.363^{+0.040}_{-0.040}$ | (*88*) |
| J0737-3039A | $1.337^{+0.005}_{-0.005}$ | (*46*) | J0737-3039B | $1.250^{+0.005}_{-0.005}$ | (*46*) |

Mean = 1.34 $M_\odot$, weighted mean = 1.41 $M_\odot$

Lattimer & Prakash (2004)

# Neutron star mass determination by Hulse & Taylor (contd.)

Observed decrease in the orbital period was successfully explained by emission of gravitational waves predicted by general relativity.

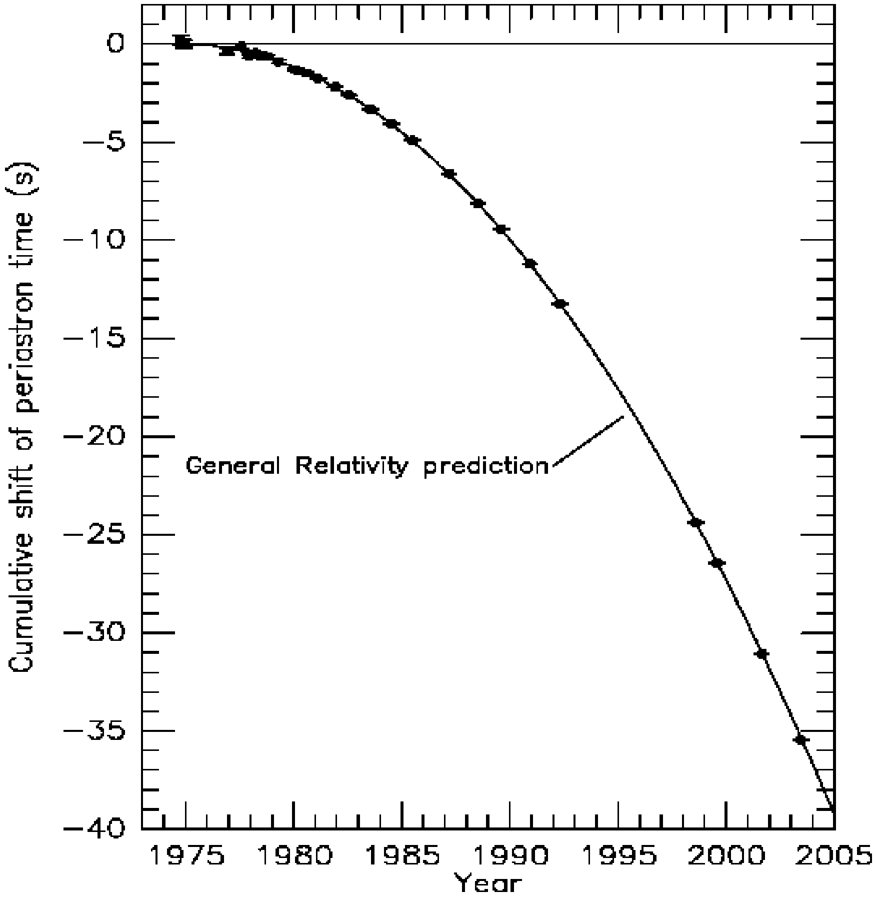


Decreasing orbital period of PSR B1913+16 (Weisberg & Taylor (2004))

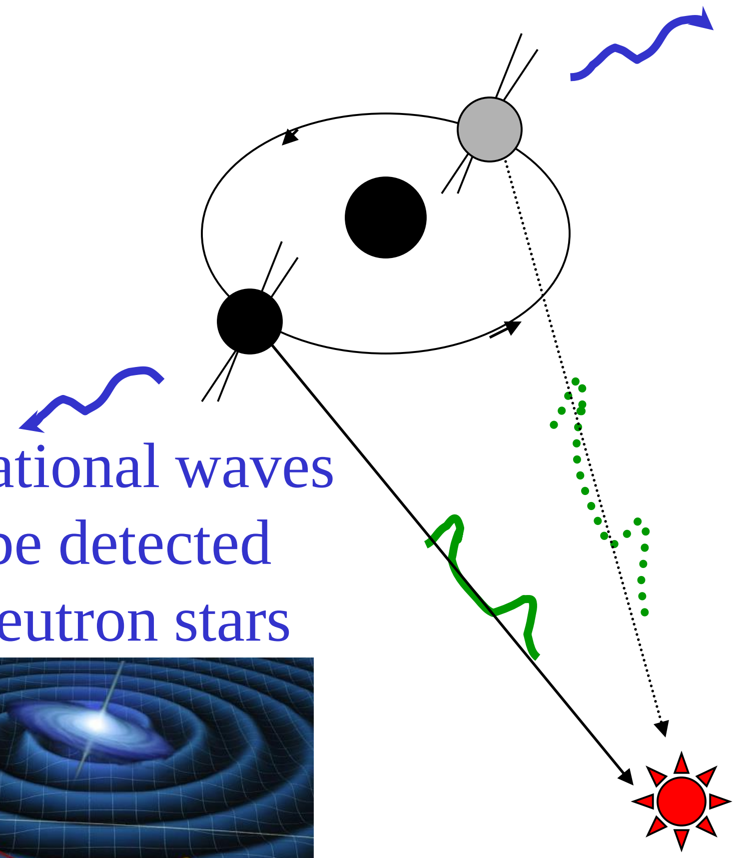

Gravitational waves yet to be detected from neutron stars

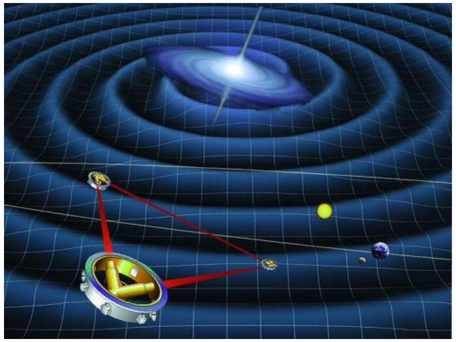

LISA project (by NASA)

# Various types of pulsars

- Double pulsar (PSR J0737-3039 alone)

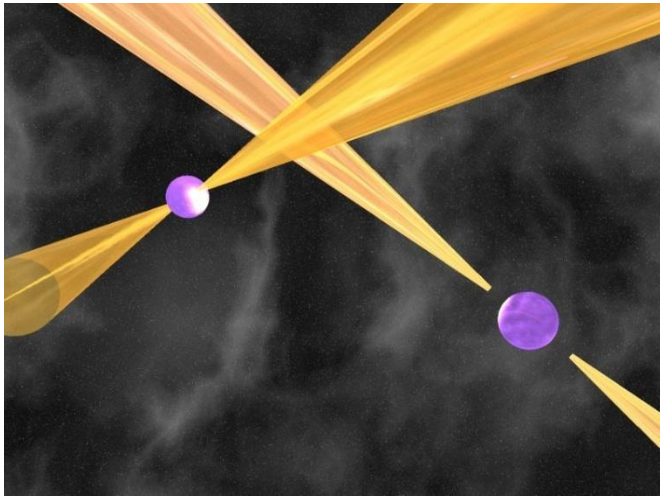

- X-ray pulsars
(accretion-powered pulsars)

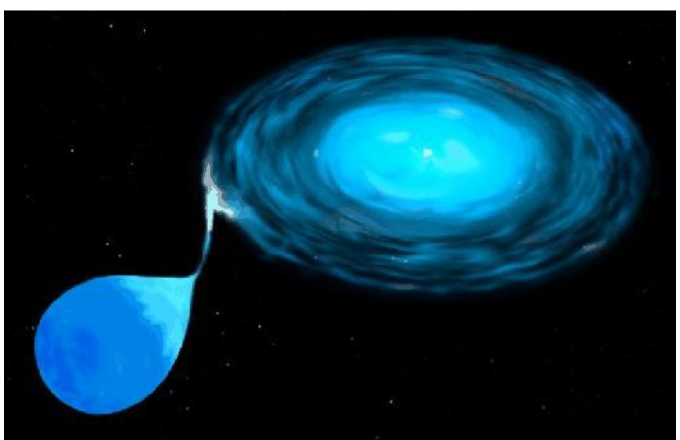

- Anomalous X-ray pulsars
(presumably, magnetars)

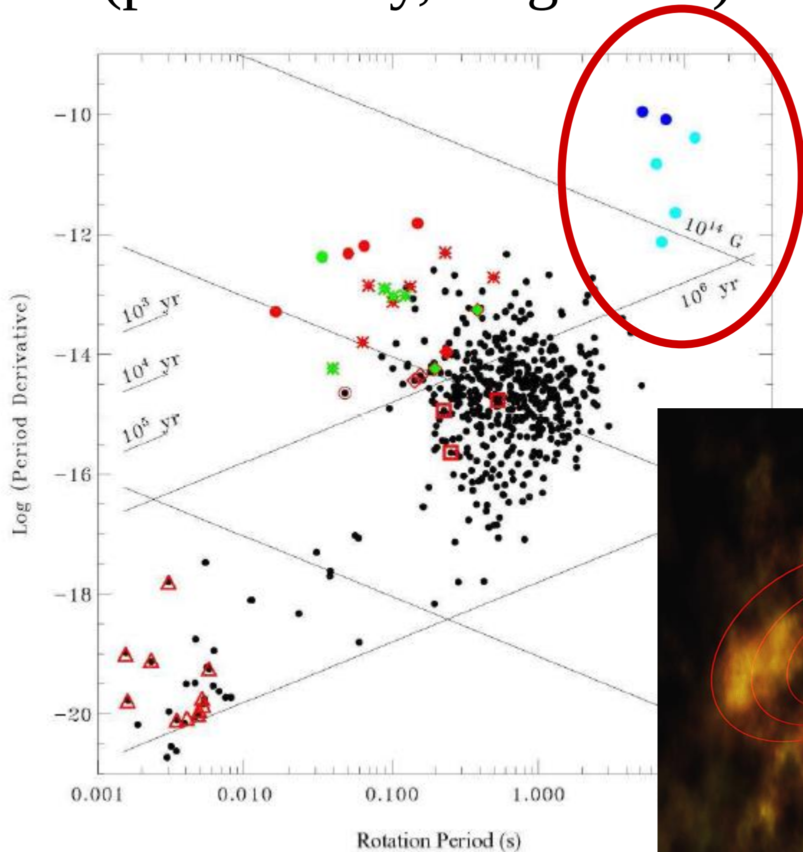


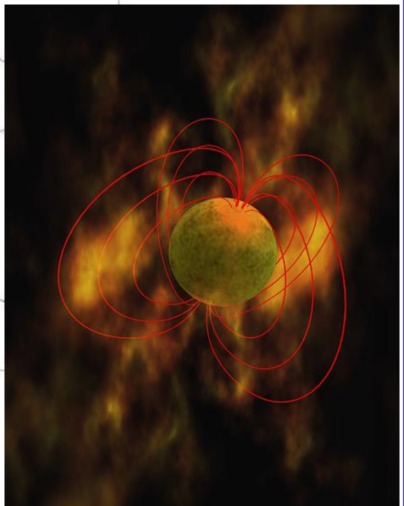

Imaginary drawing by NASA

# Neutron stars as theoretical products

- 1932: Discovery of the neutron by Chadwick via $^{9}Be + \alpha \rightarrow {}^{12}C + n$.

Just before that, Landau considered the possible presence of dense stars like one giant nucleus, and afterwards the possibility that a “neutron star” could exist due to the degeneracy pressure of neutrons of density higher than normal nuclear density.


- 1934: W. Baade and F. Zwicky, Phys. Rev. **45**, 138 (1934).

… With all reserve we advance the view that supernovae represent the transitions from ordinary stars into ***neutron stars***, which in their final stages consist of extremely closely packed neutrons.

# Observed masses

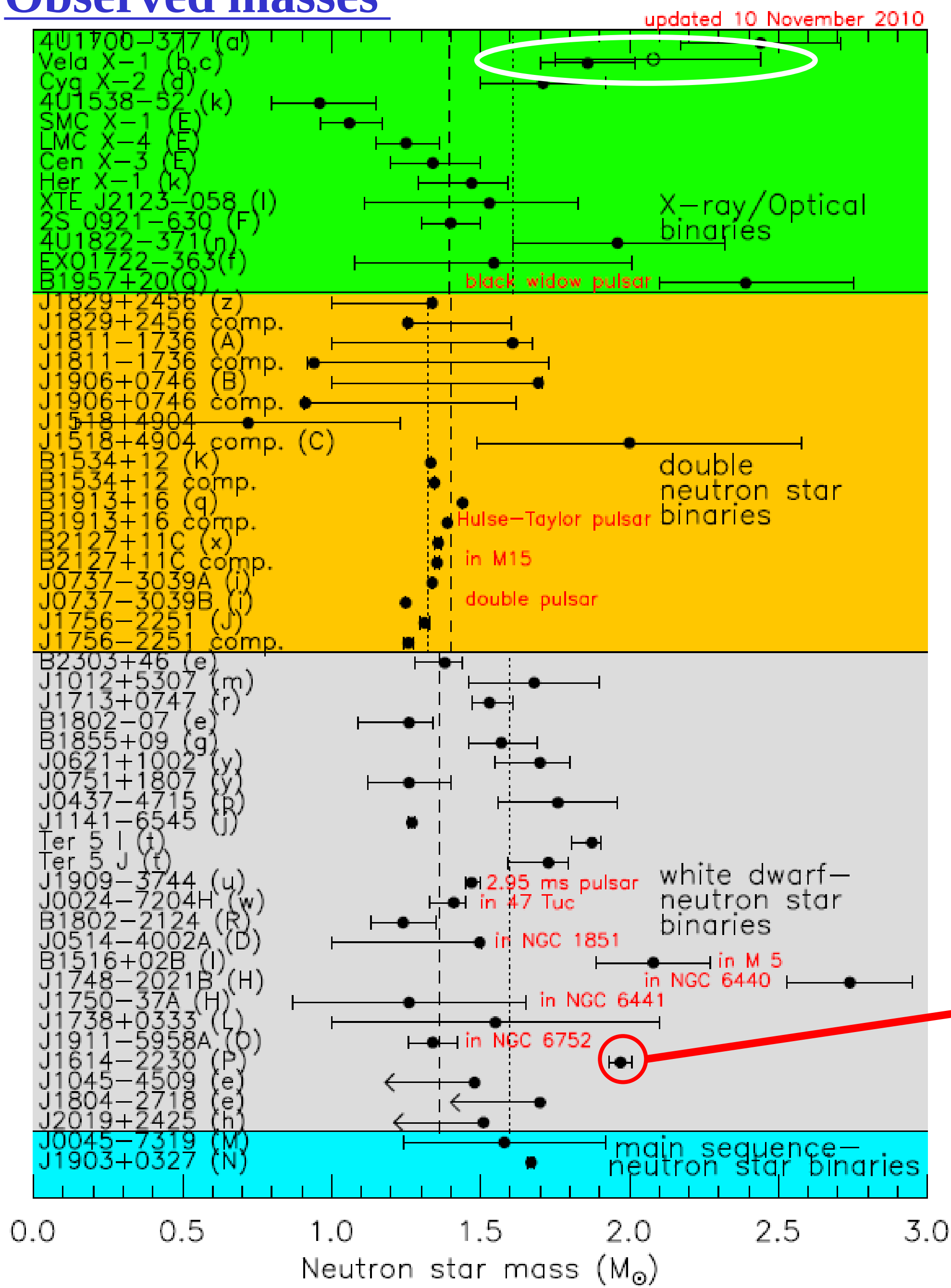


Lattimer & Prakash, arXiv:1012.3208.

## Pulsar twice as heavy as the Sun

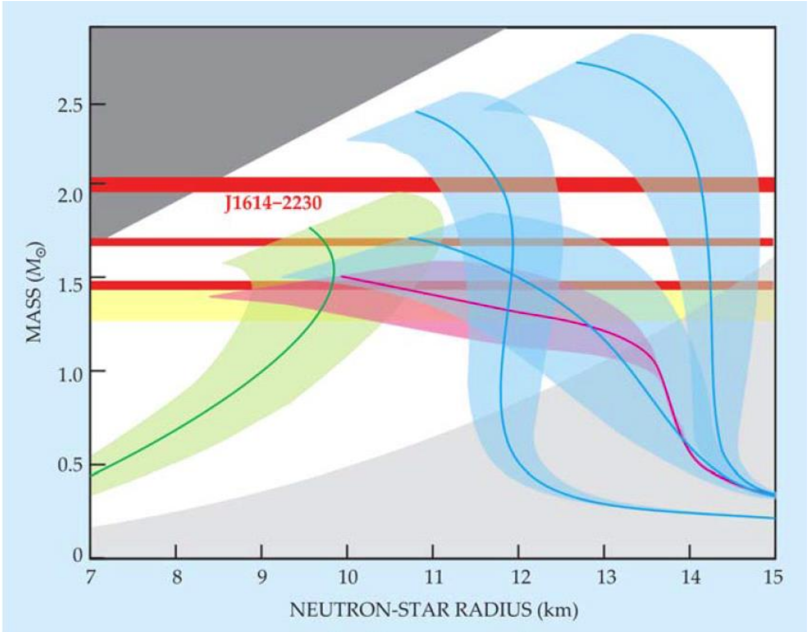


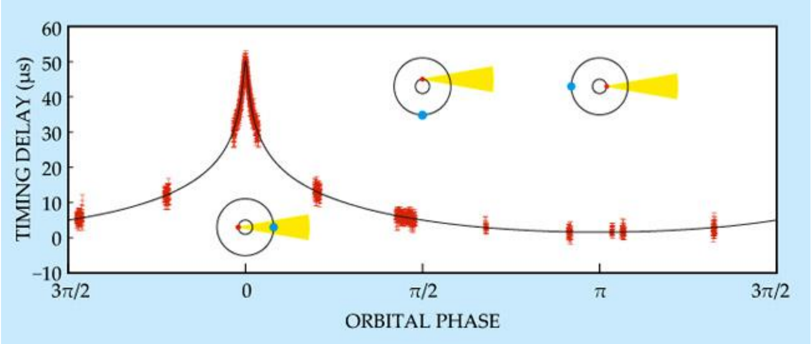


Demorest et al. (2010)

# The Best Measured Neutron Star Radii

$R_\infty < 5\%$

| Name | $R_\infty$ (km/D) | D (kpc) | $kT_{eff,\infty}$ (eV) | $N_H$ ($10^{20}$ cm$^{-2}$) | Ref. |
|---|---|---|---|---|---|
| omega Cen (Chandra) | 13.5 ± 2.1 | 5.36 ±6% | $66^{+4}_{-5}$ | (9) | Rutledge et al (2002) |
| omega Cen** (XMM) | 13.6 ± 0.3 | 5.36 ±6% | 67 ±2 | 9 ± 2.5 | Gendre et al (2002) |
| M13** (XMM) | 12.6 ± 0.4 | 7.80 ±2% | 76 ±3 | (1.1) | Gendre et al (2002) |
| 47 Tuc X7 (Chandra) | $34^{+22}_{-13}$ | 5.13 ±4% | $84^{+13}_{-12}$ | $0.13^{+0.06}_{-0.04}$ | Heinke et al (2006) |
| M28** (Chandra) | $14.5^{+6.9}_{-3.8}$ | 5.5 ±10% | $90^{+30}_{-10}$ | 26 ± 4 | Becker et al (2003) |
| M30 (Chandra) | $16.9^{+5.4}_{-4.3}$ | -- | $94^{+17}_{-12}$ | $2.9^{+1.7}_{-1.2}$ | Lugger et al (2006) |
| NGC 2808 (XMM) | ?? | 9.6 (?) | $103^{+18}_{-33}$ | $18^{+11}_{-7}$ | Webb et al (2007) |

Caveats:

- All IDd by X-ray spectrum (47 Tuc, Omega Cen now have optical counterparts)
- calibration uncertainties

Distances:
Carretta et al (2000),
Thompson et al (2001)

**Quiescent low-mass X-ray binaries in globular clusters**

Apparent radius:

$$R_\infty = \frac{R}{\sqrt{1 - 2GM/Rc^2}}$$

Distance to the globular cluster

Rutledge (2010)

# Neutron star matter

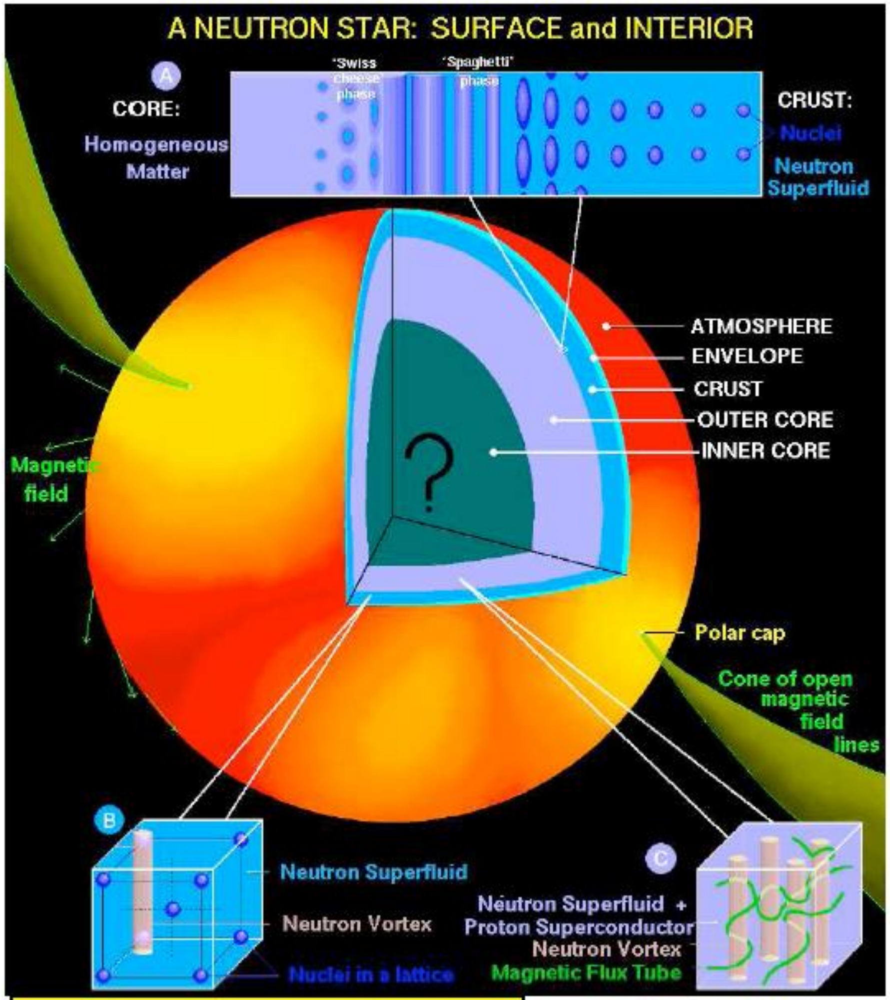


Lattimer and Prakash, astro-ph0405262

Figure by D. Page

# Schematic phase diagram of dense matter

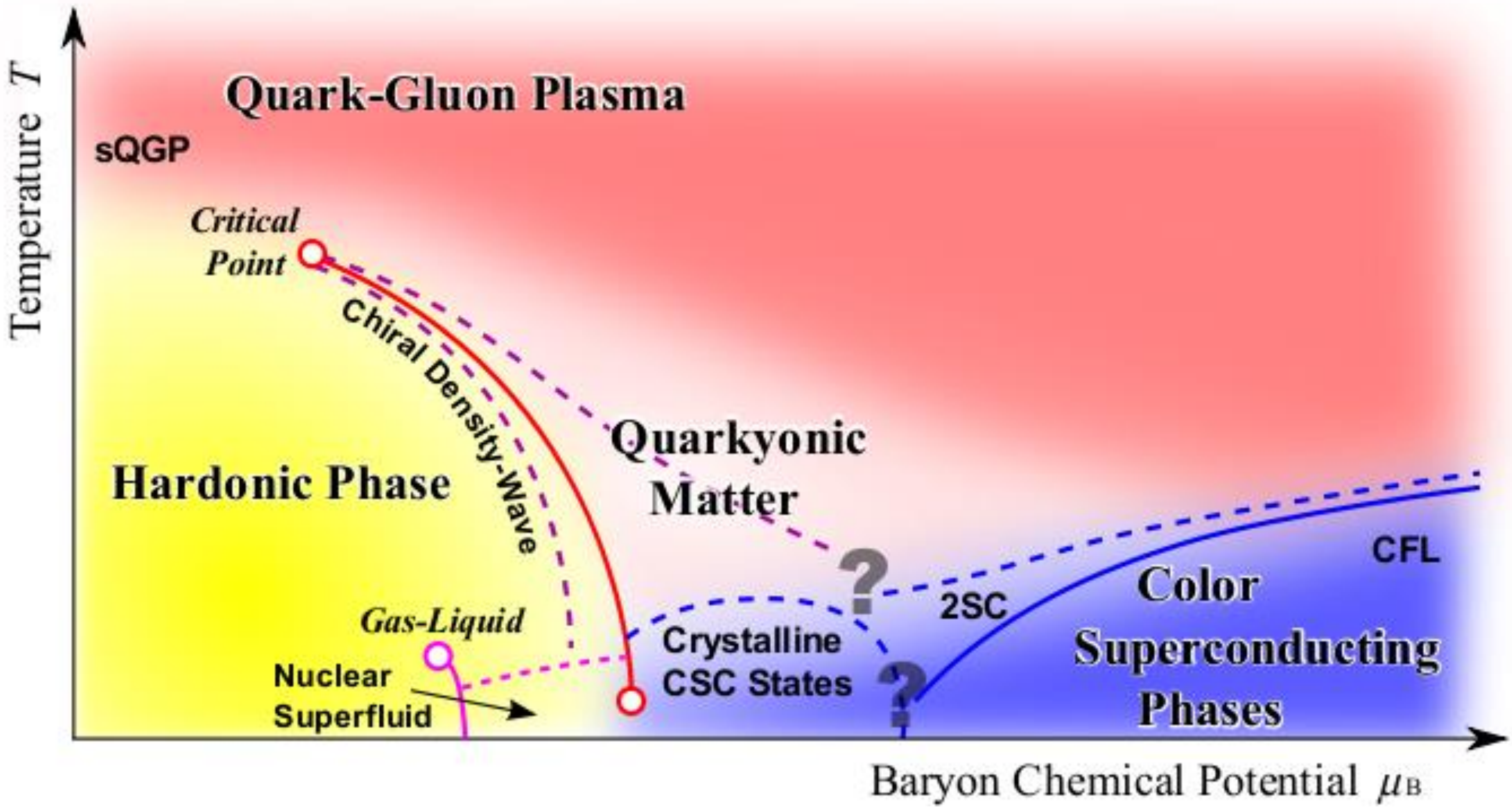


By Fukushima

# Systems composed of nuclear matter

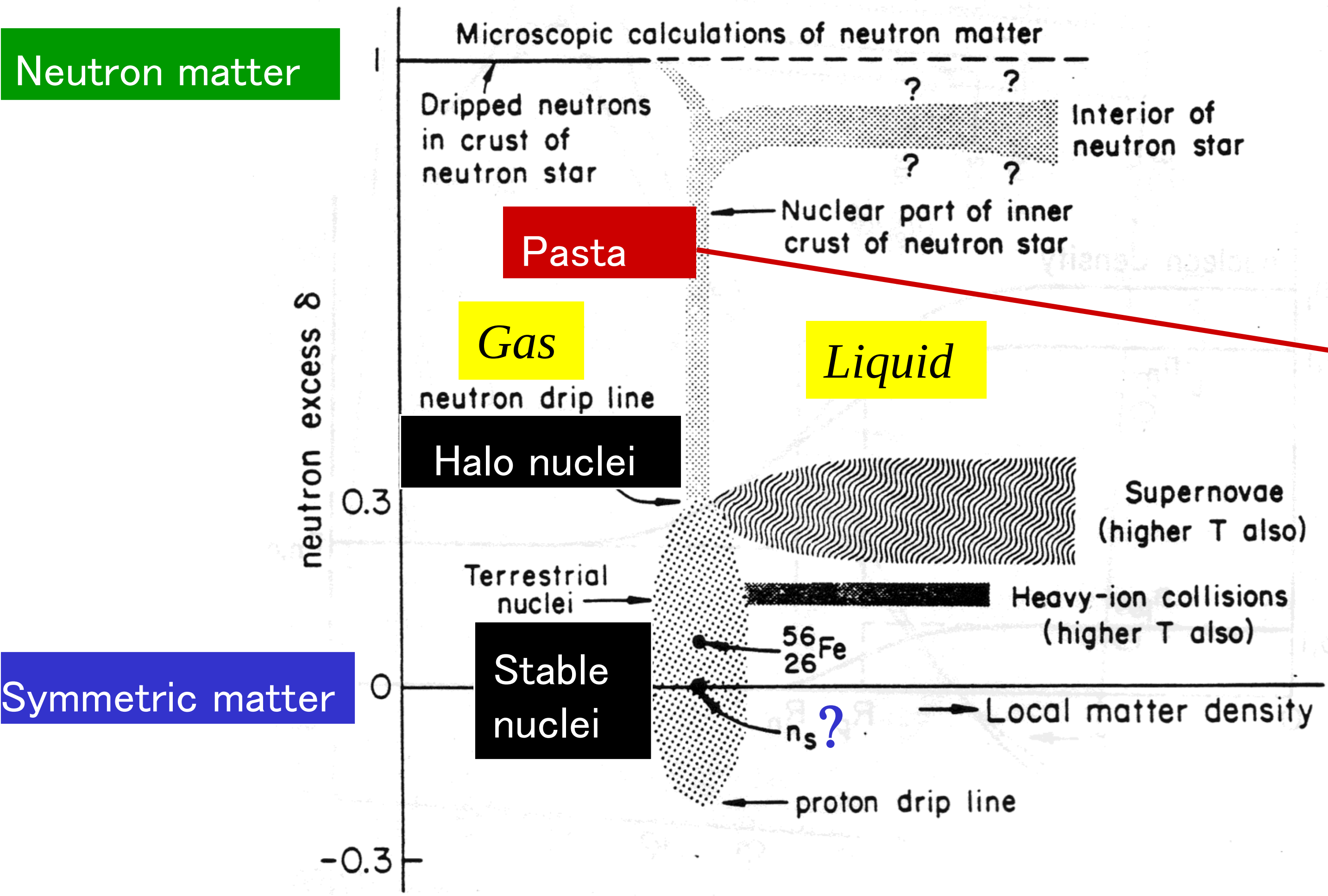


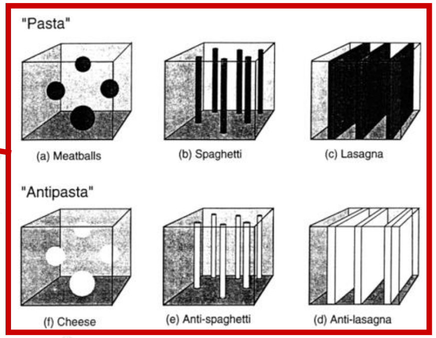


From Lamb (1991).

Pethick & Ravenhall, ARNPS **45** (1995) 429.

# Microscopic EOS calculations

*Pure neutron matter*

Scattering length $a \approx$-18 fm
Effective range $R \approx$2 fm

Green's function Monte-Carlo (GFMC) with Argonne $v_8$'

$0.5E_{FG}/N$

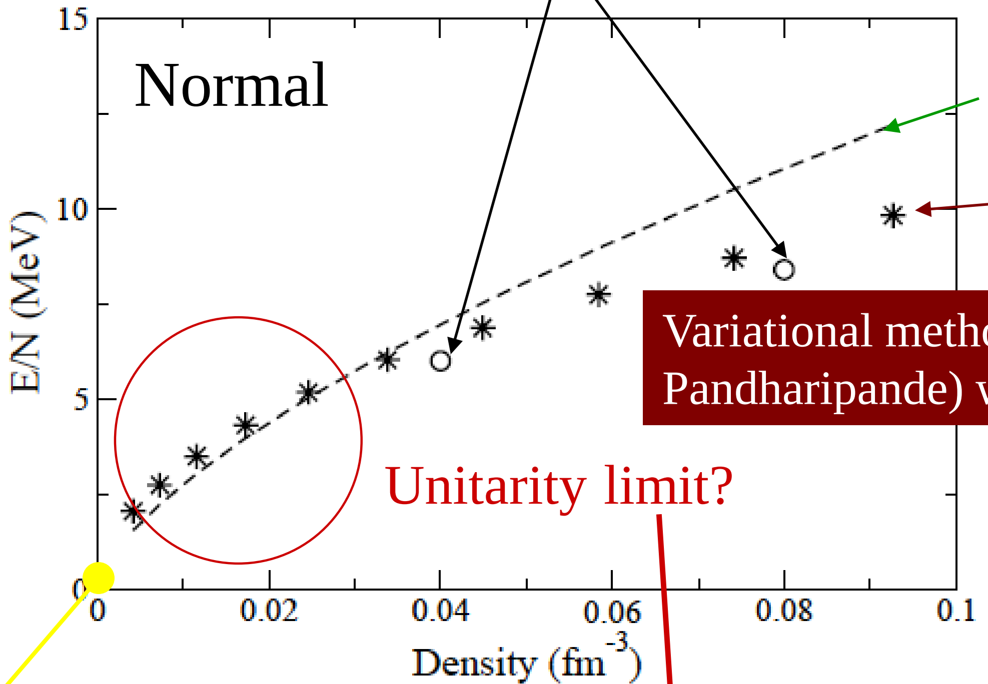


Variational method (Friedman-Pandharipande) with Urbana $v_{14}$+TNI

Unitarity limit?

Low-density expansion:

$$E = E_{FG}\left[1+\frac{10}{9\pi}k_F a+\frac{4}{21\pi^2}(11-2\ln 2)(k_F a)^2+\cdots\right]$$

Ref. Carlson et al., PRC **68** (2003) 025802.

$|a| >> k_F^{-1} >> R$

# Microscopic EOS calculations (contd.)

*Pure neutron matter*

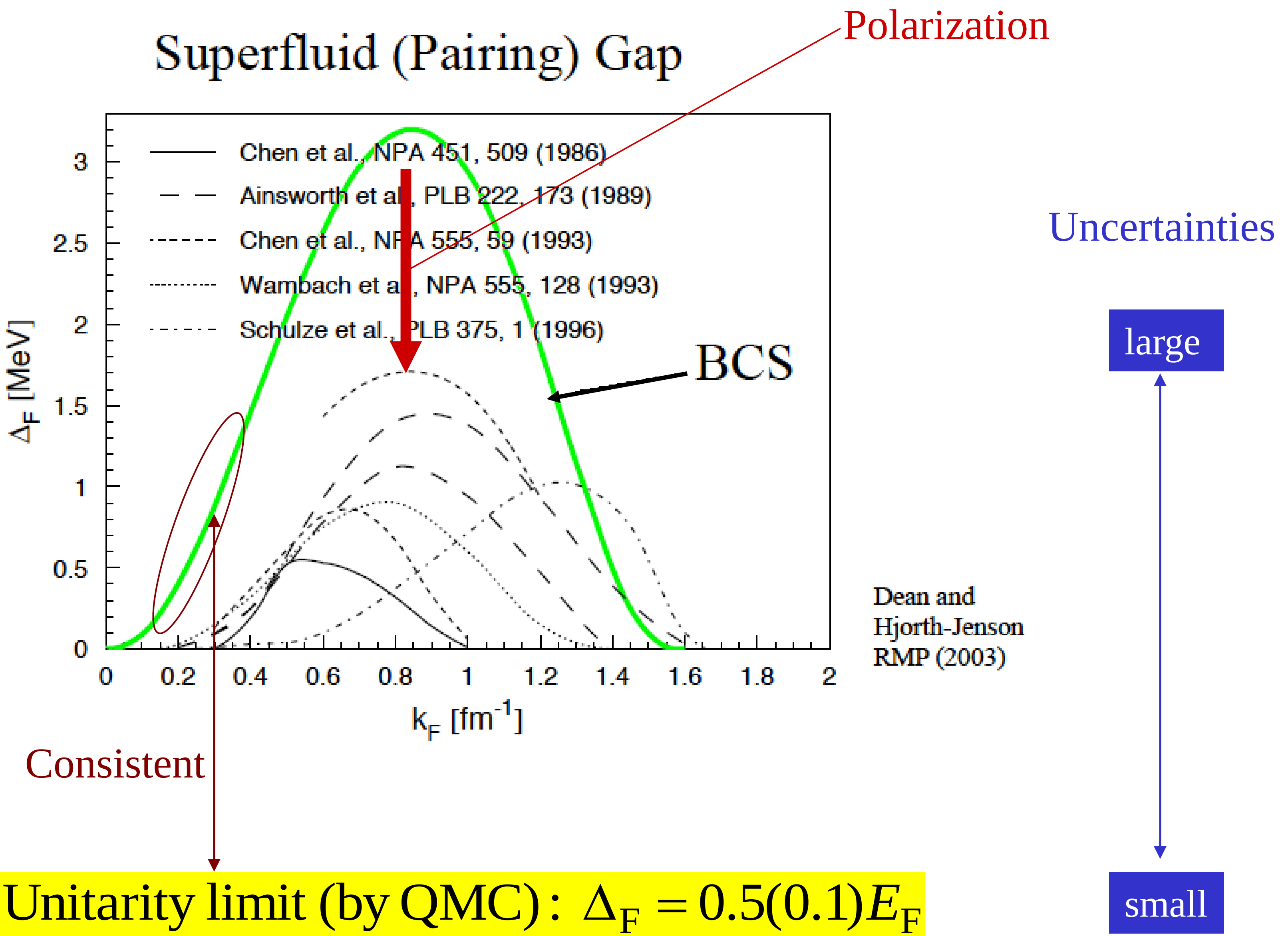


$$\text{Unitarity limit (by QMC)}: \ \Delta_F = 0.5(0.1)E_F$$

Ref. Carlson and Reddy, PRL **95** (2005) 060401.

# Nuclear matter in neutron stars

*Schematic cross-section of a neutron star*

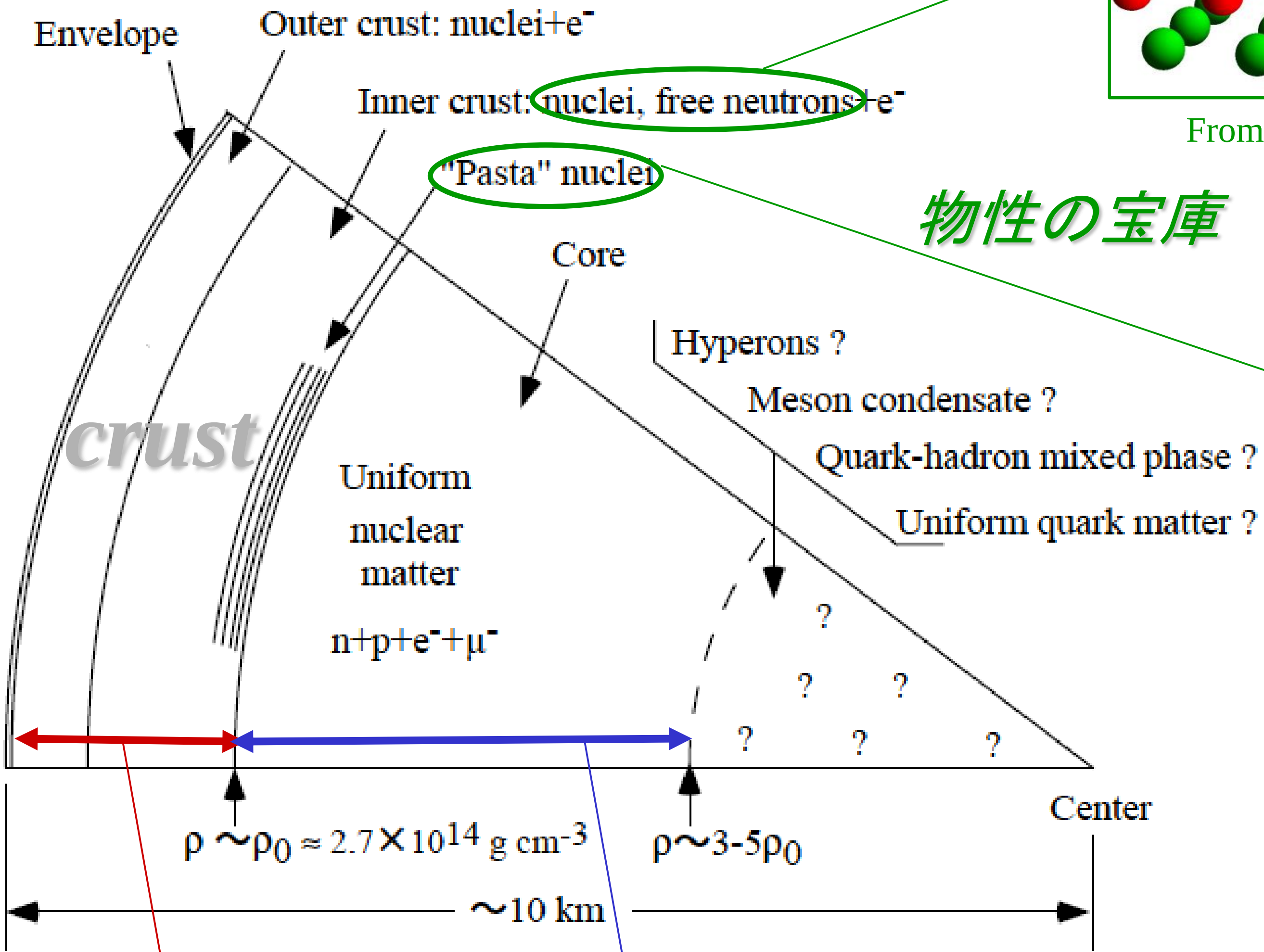


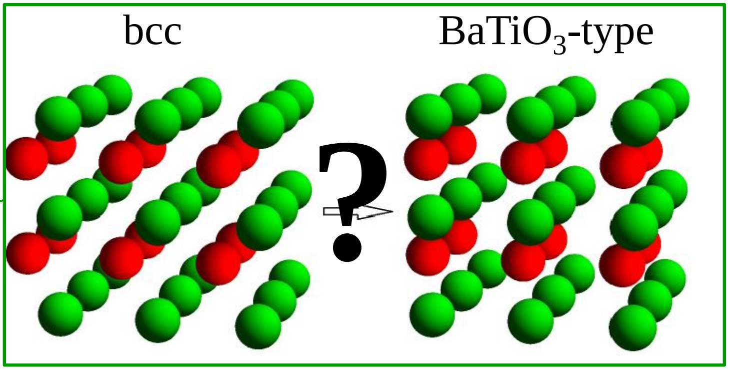


From Kobyakov and Pethick (2013, 2016).

*物性の宝庫*

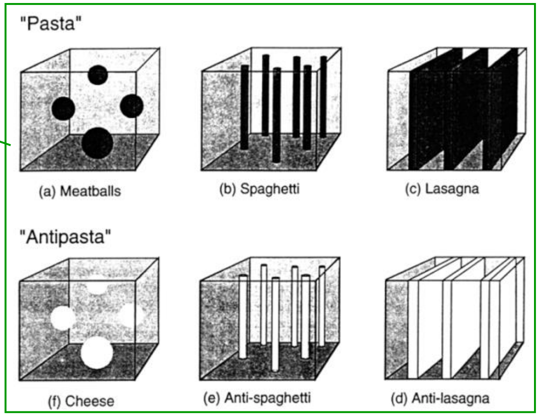


From Lamb (1991).

Liquid-gas mixture

Liquid

$T < \sim 10^9$ K (cold)

# Neutron matter and trapped cold atoms

## *Low density neutron matter*

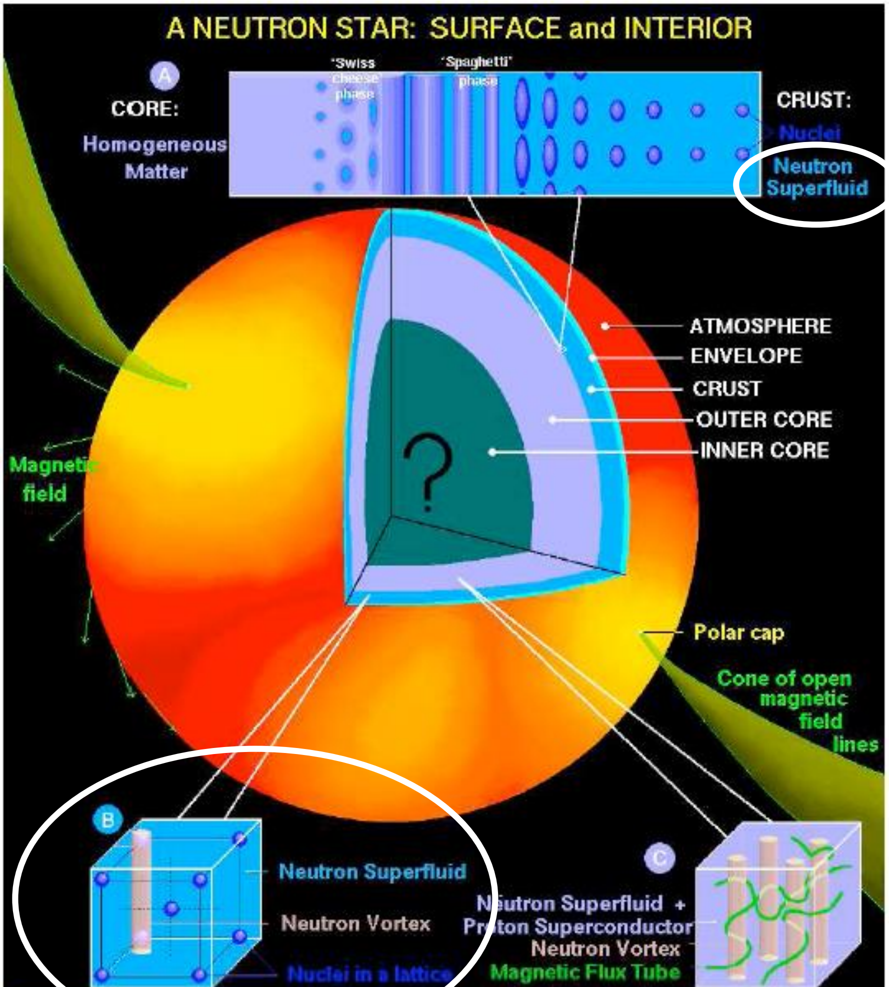


Lattimer and Prakash, astro-ph0405262

Figure by D. Page

## *Cold Fermi atoms near Feshbach resonance*

**Universal Interaction Energy at Unitarity**

*In-situ* absorption images

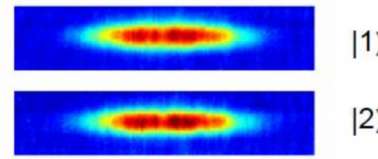


*Size* of real space distribution reveals interaction and pairing energies

At unitarity, the chemical potential is reduced by pairing: $\mu = E_F(1+\beta)^{1/2}$

where $\beta$ is a *universal* many-body parameter $\beta = -0.54 \pm 0.05$

From R. Hulet.

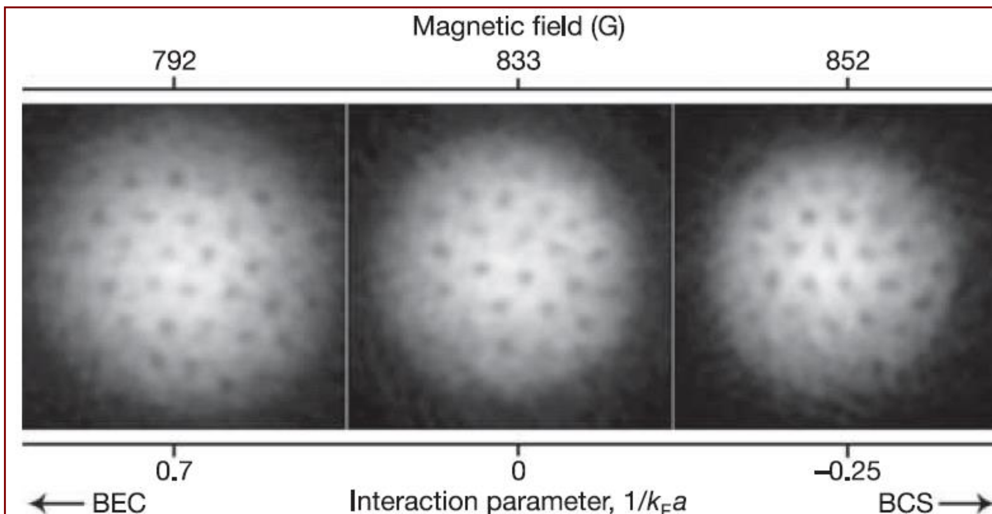


From M.W. Zwierlein.

# Effects of superfluidity

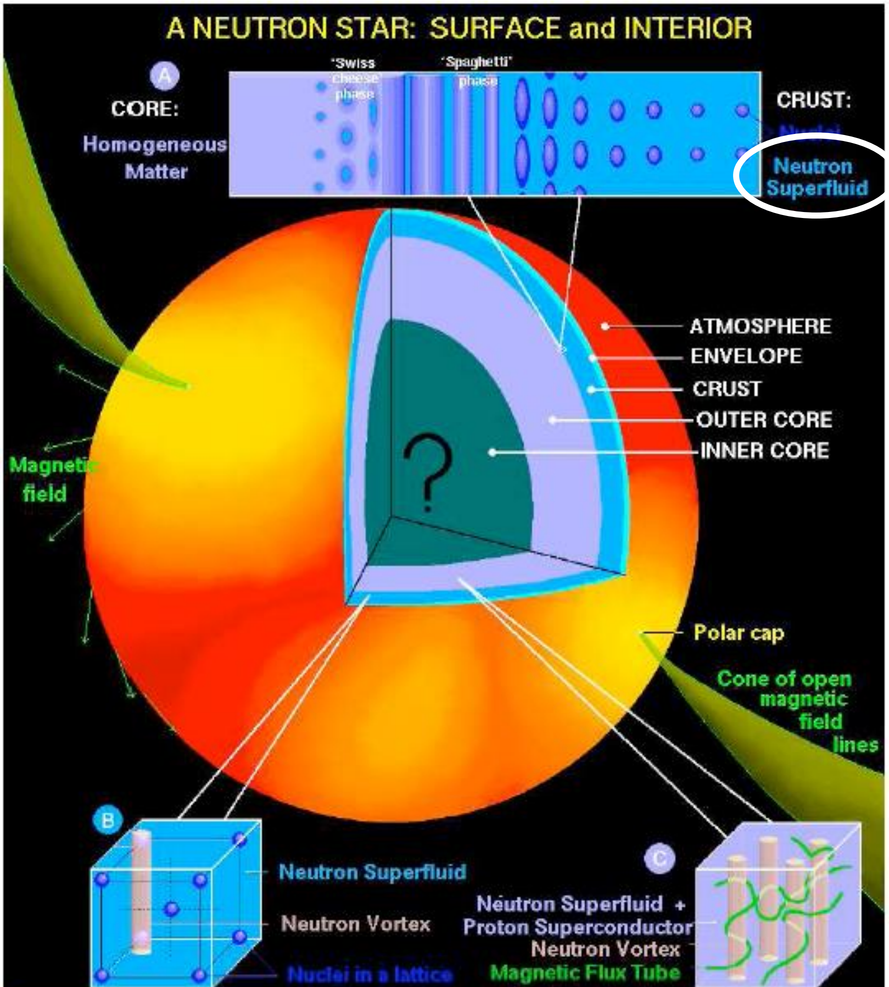


Lattimer and Prakash, astro-ph0405262

Figure by D. Page

## *Neutron band structure*

crust uniform

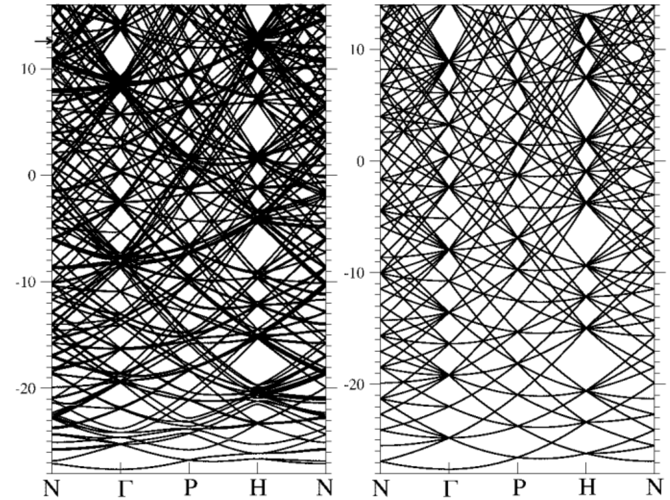


Chamel (2012).

## *Torsional oscillation frequency*

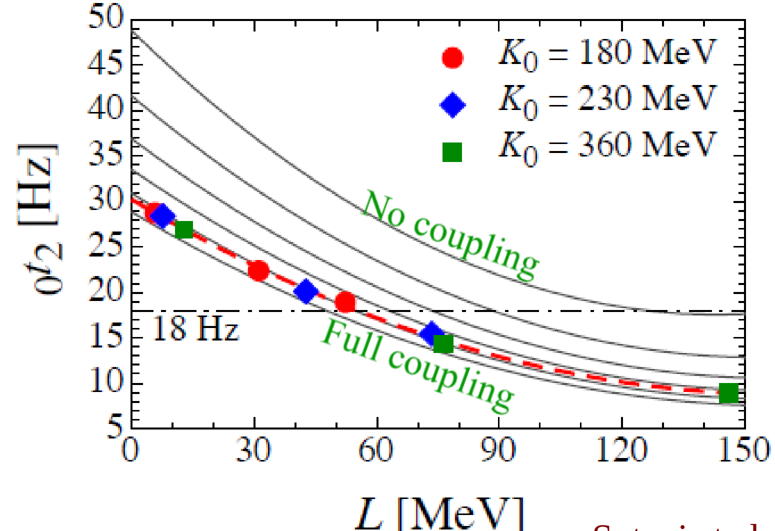


Sotani et al. (2012).

***Superfluid neutrons are coupled with a lattice of nuclei.***

# QPOs in giant flares from soft-gamma repeaters (SGRs)

Magnetars

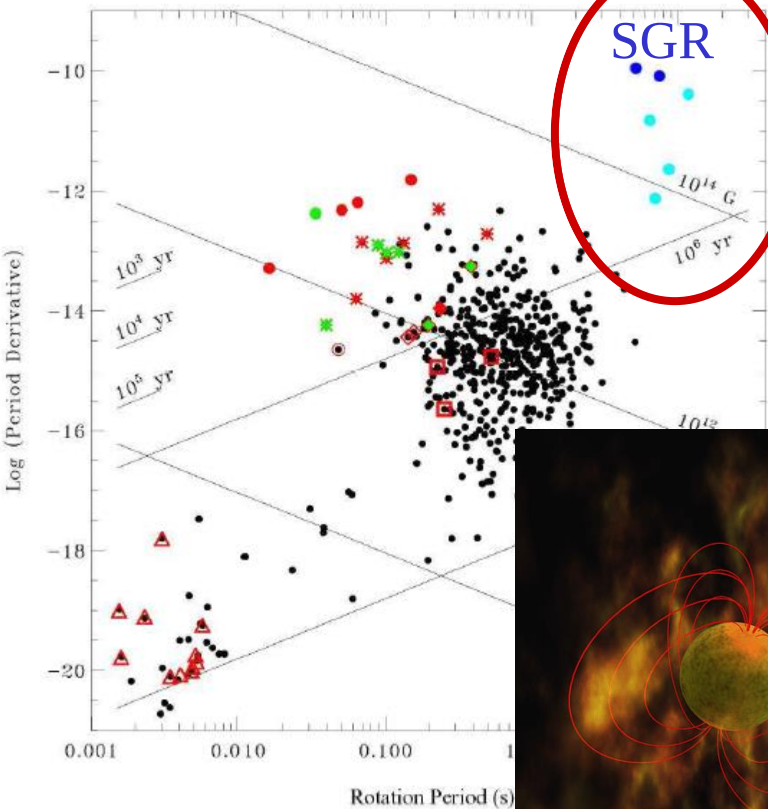


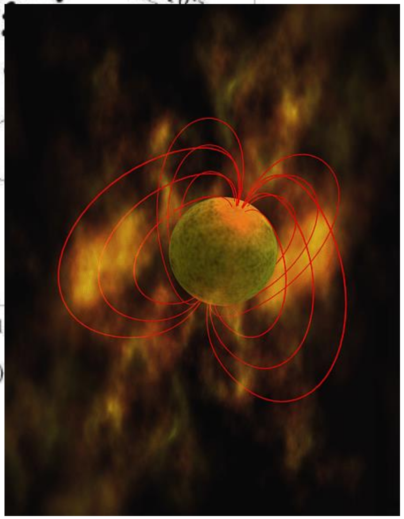

arXiv:astro-ph/0208356

image by NASA

X-ray light curve of the SGR 1806-20 giant flare

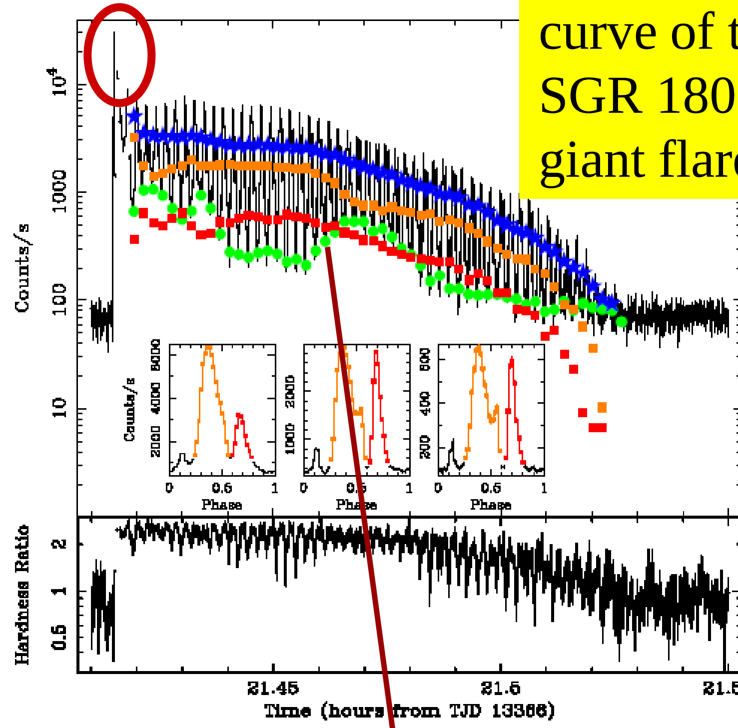


QPOs

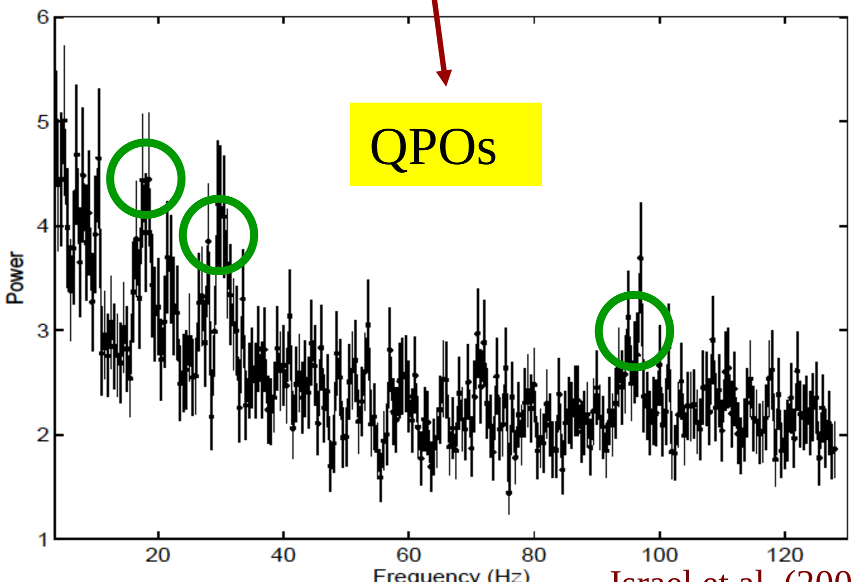


Israel et al. (2005)

# Nuclear pasta as liquid crystals

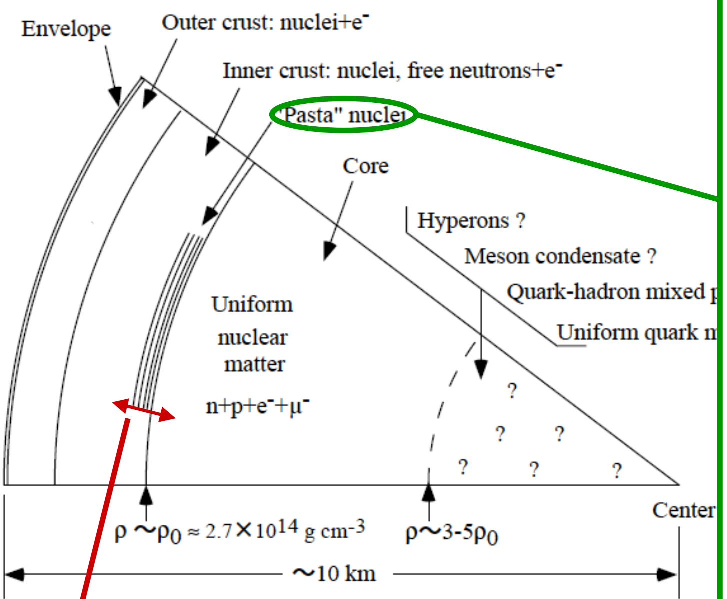


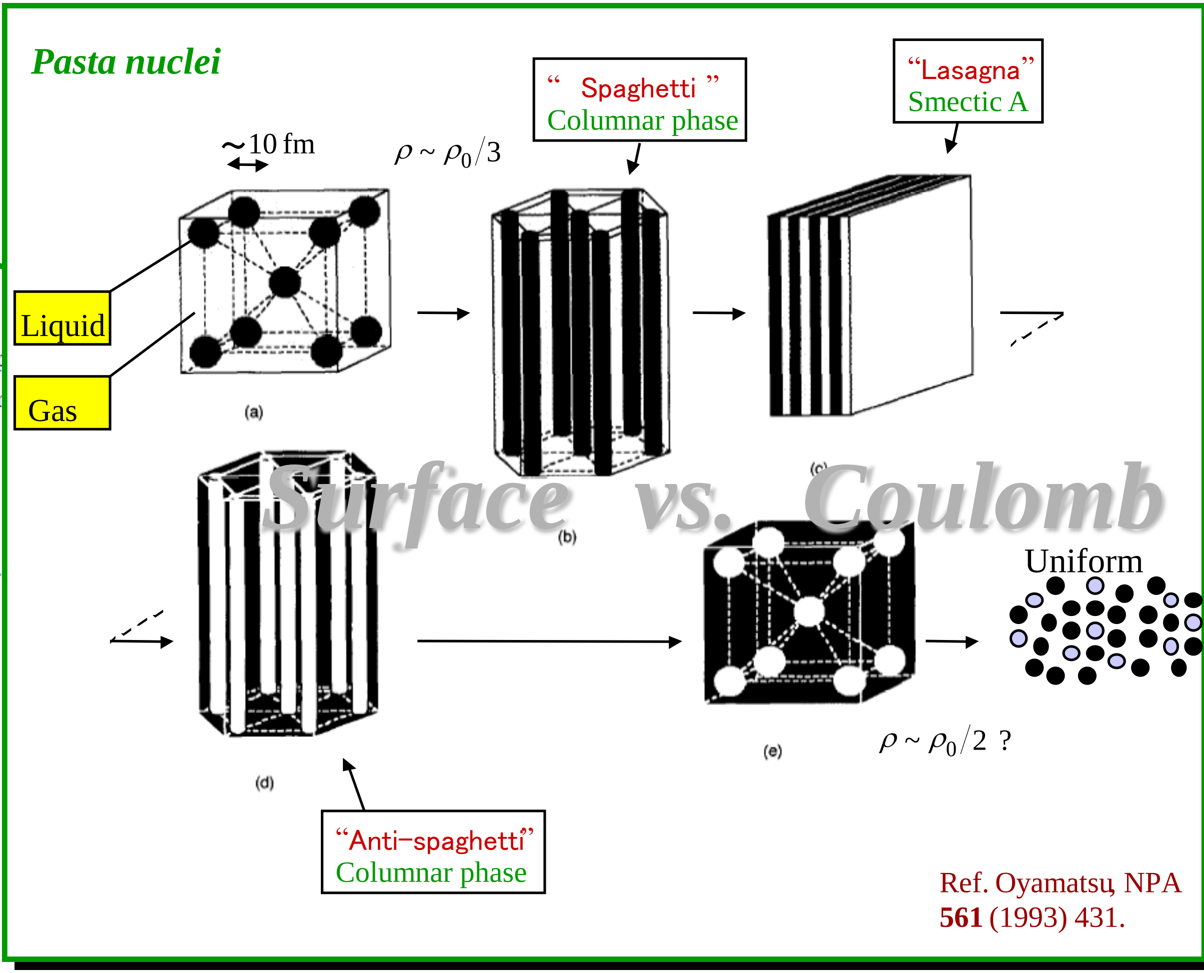


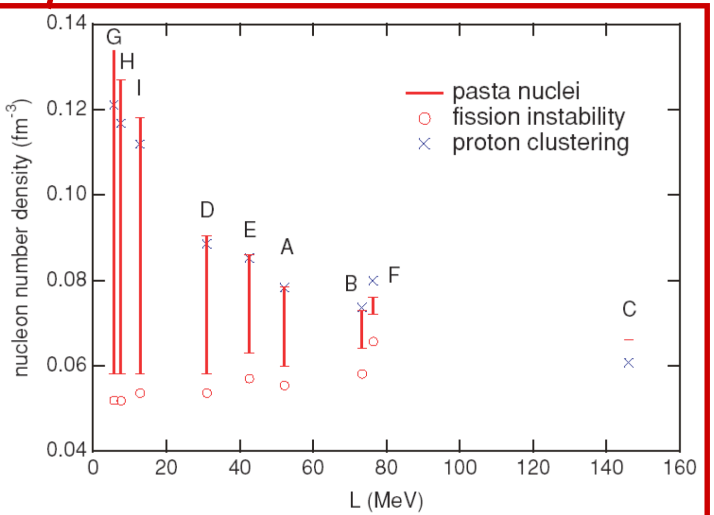


The larger *L*, the narrower pasta region.

Ref. Oyamatsu & Iida, PRC **75** (2007) 015801.

# Pasta structure in cuprates

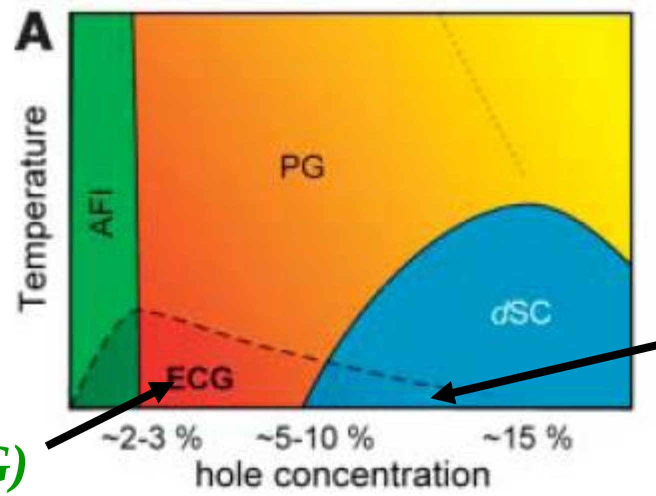


*Stripes*

*Electronic cluster glass (ECG)*

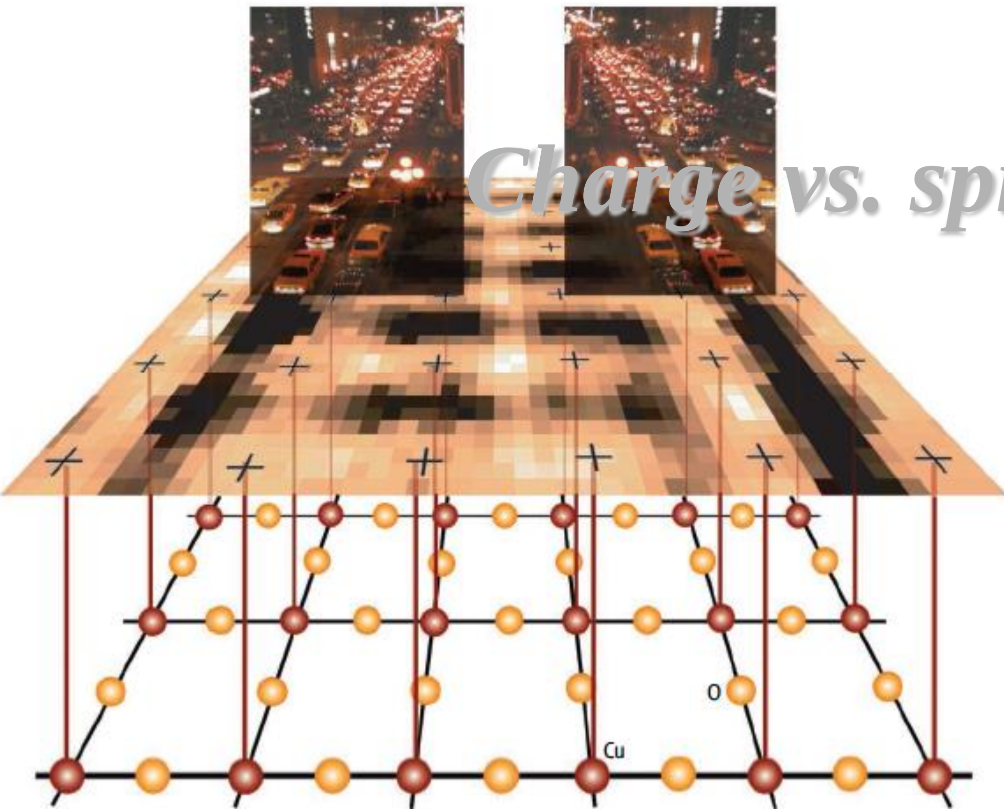


**Charge vs. spin vs. orbit vs. lattice**

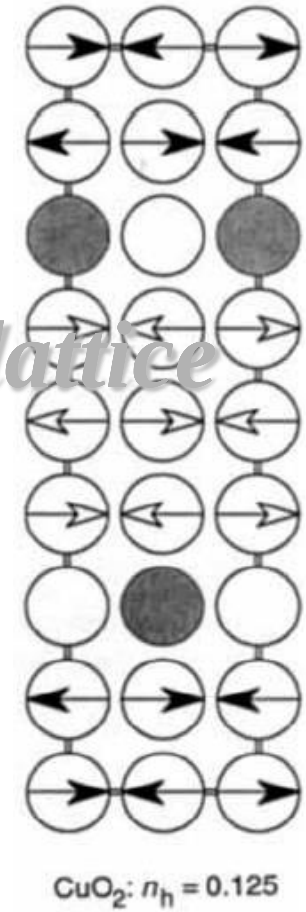


Refs. Kohsaka et al., Science **315** (2007) 1380; Tranquada et al., Nature **375** (1995) 561.

# Gyroid in nuclear pasta

Ref. Nakazato, Iida, & Oyamtasu, arXiv:1011.3866.

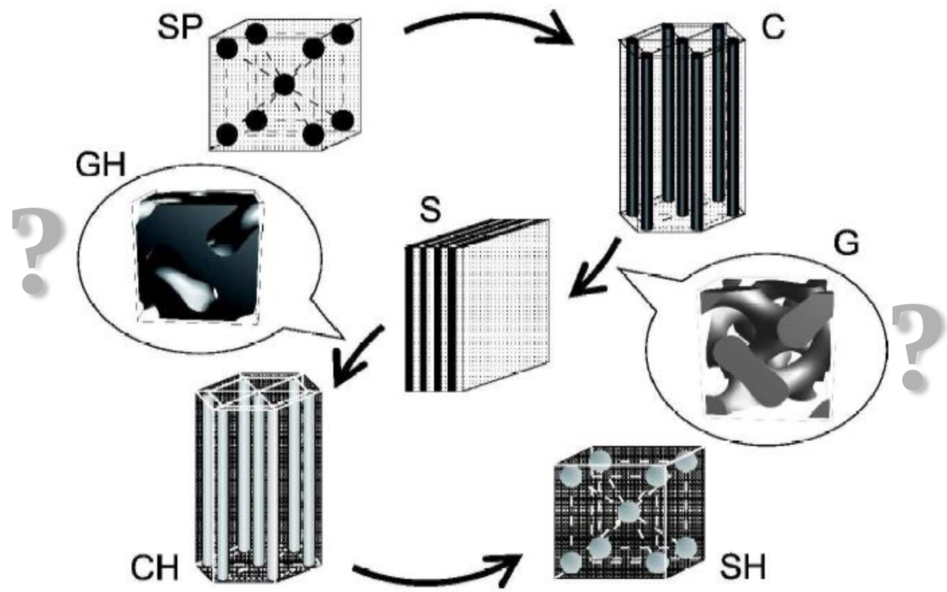


**Curvature corrections (proton fraction=0.3)**

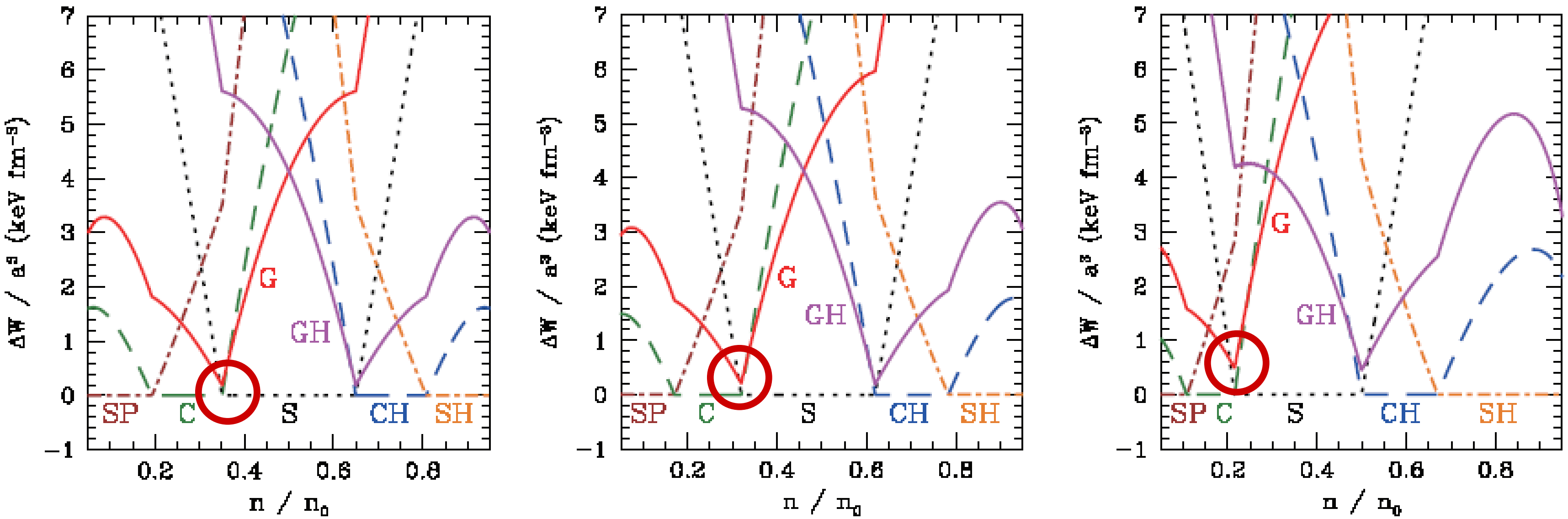

# Gyroid in polymer systems

Ref. Bates & Fredrickson, Phys. Today Feb. (1999)32.

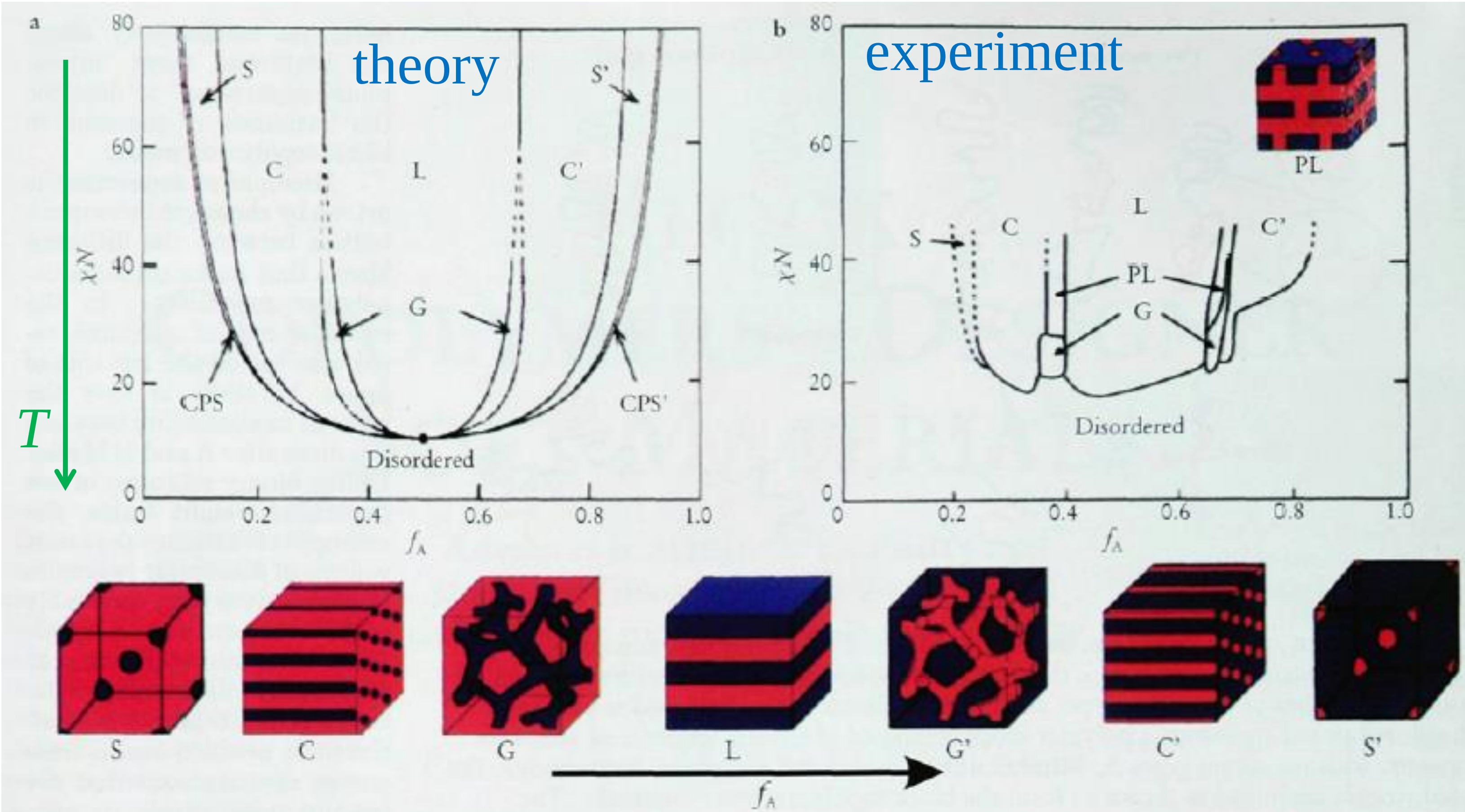


FIGURE 3. PHASE DIAGRAM for linear AB diblock copolymers, comparing theory and experiment. **a:** Self-consistent mean-field theory[8] predicts four equilibrium morphologies: spherical (S), cylindrical (C), gyroid (G) and lamellar (L), depending on the composition $f$ and combination parameter $\chi N$. Here, $\chi$ is the segment–segment interaction energy (proportional to the heat of mixing A and B segments) and $N$ is the degree of polymerization (number of monomers of all types per macromolecule). **b:** Experimental phase portrait for poly(isoprene-styrene) diblock copolymers.[9] The resemblance to the theoretical diagram is remarkable, though there are important differences, as discussed in the text. One difference is the observed PL phase, which is actually metastable. Shown at the bottom of the figure is a representation of the equilibrium microdomain structures as $f_A$ is increased for fixed $\chi N$, with type A and B monomers confined to blue and red regions, respectively.

# Metastable gyroid in proto-neutron stars

Ref. Schuetrumpf et al. arXiv:1404.4760.

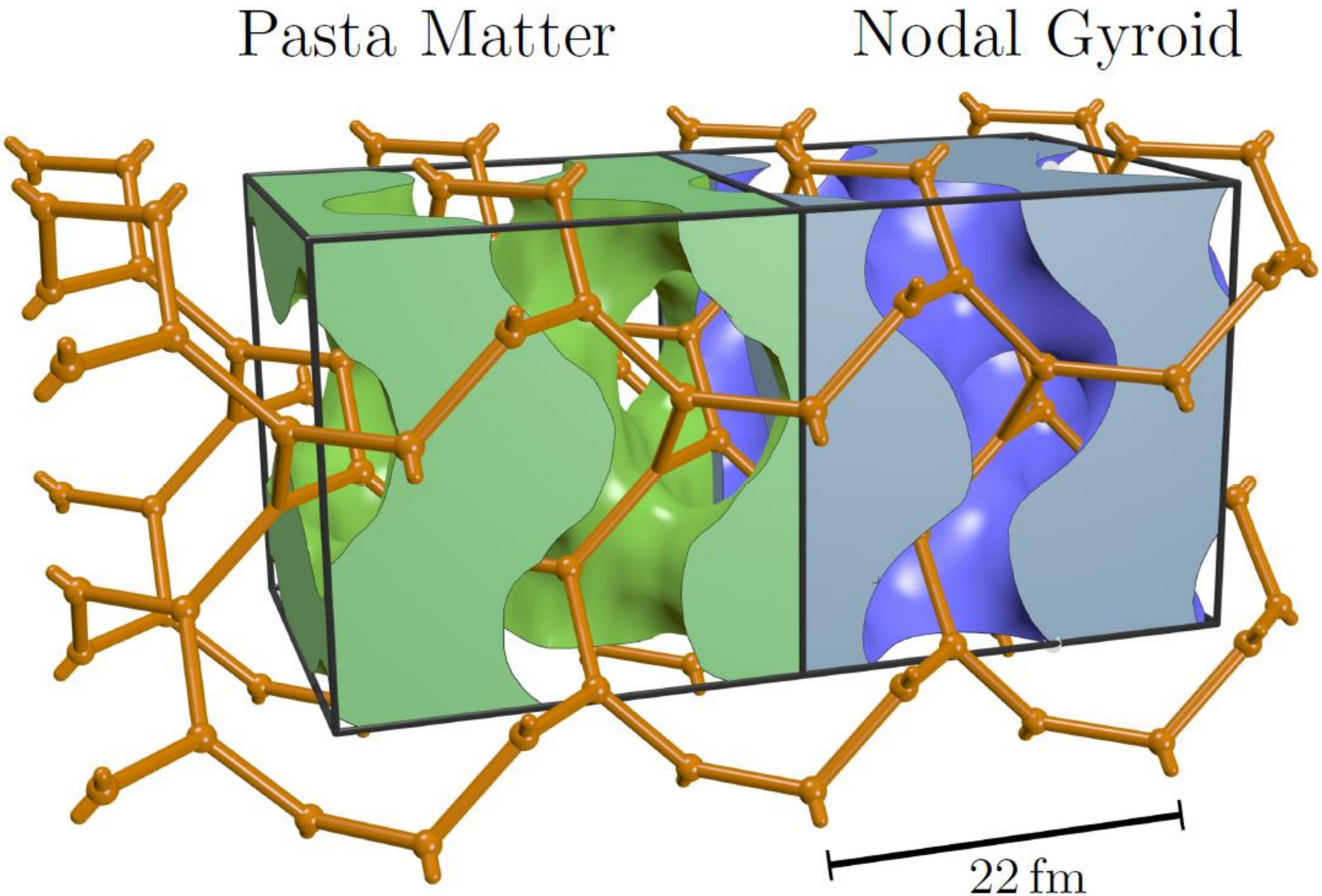


Time dependent Hartree-Fock calculations for supernova matter at temperature 7 MeV and density 0.06 $fm^{-3}$

# Phenomenological EOS parameters

Energy per nucleon of bulk nuclear matter near the saturation point (nucleon density $n$, neutron excess $\alpha$):

$$w = w_0 + \frac{K_0}{18n_0^2}(n-n_0)^2 + \left[S_0 + \frac{L}{3n_0}(n-n_0)\right]\alpha^2$$

| | |
|---|---|
| $n_0, w_0$ | saturation density & energy of symmetric nuclear matter |
| $S_0$ | symmetry energy coefficient |
| $K_0$ | incompressibility |
| $L$ | density symmetry coefficient |

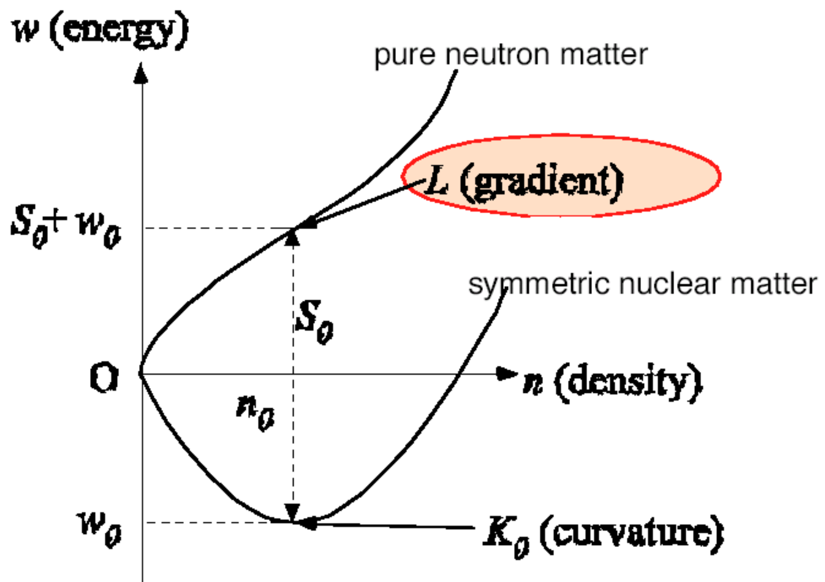

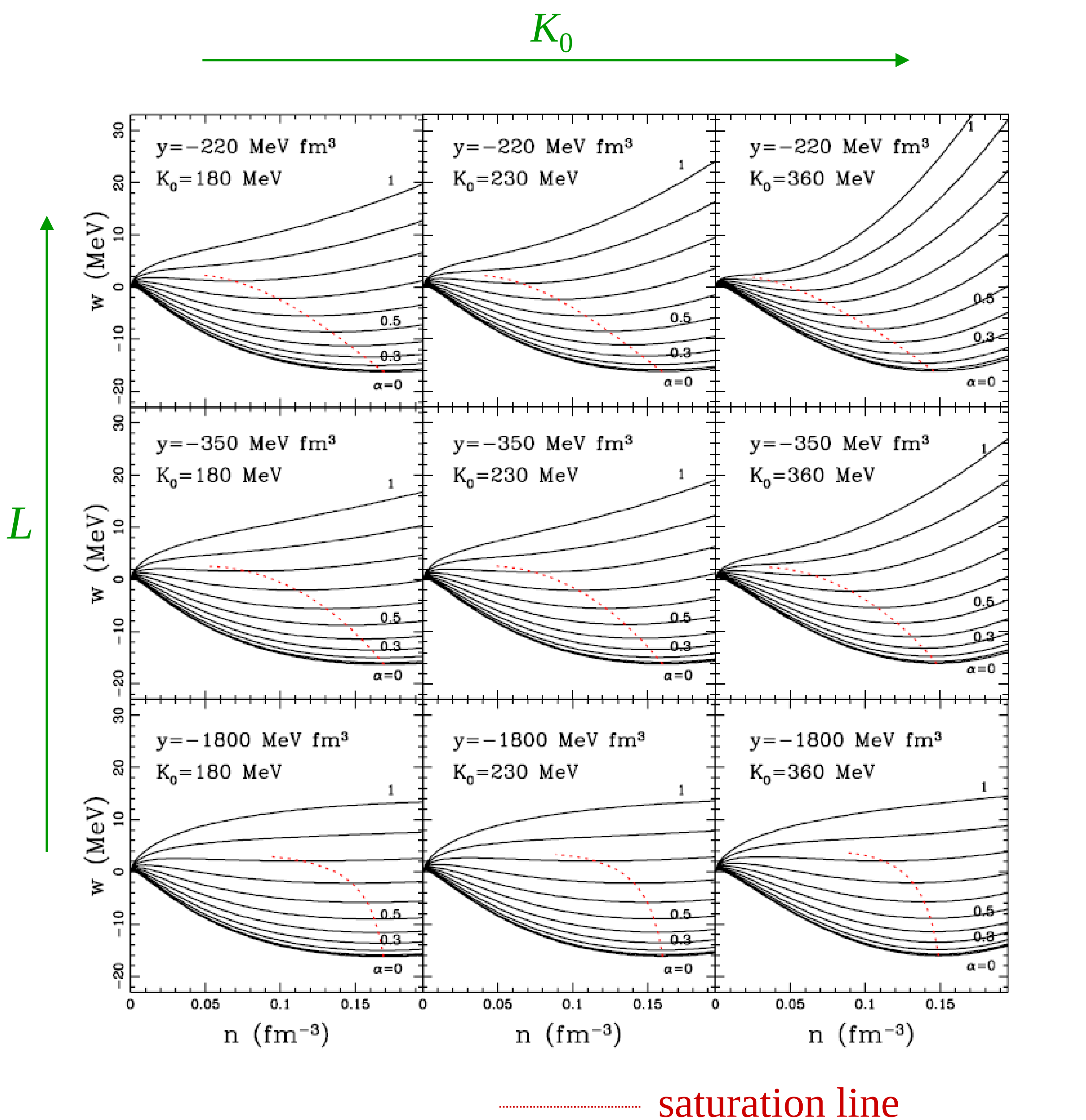


($y$=-$K_0S_0/3n_0L$ : slope at $\alpha$=0)

Ref. Oyamatsu & Iida, PTP **109**(2003)631.

# Recently, measured masses and radii have been accumulated.

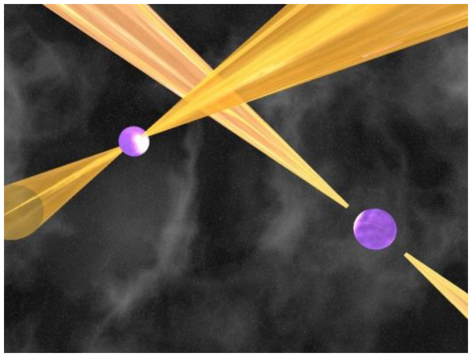

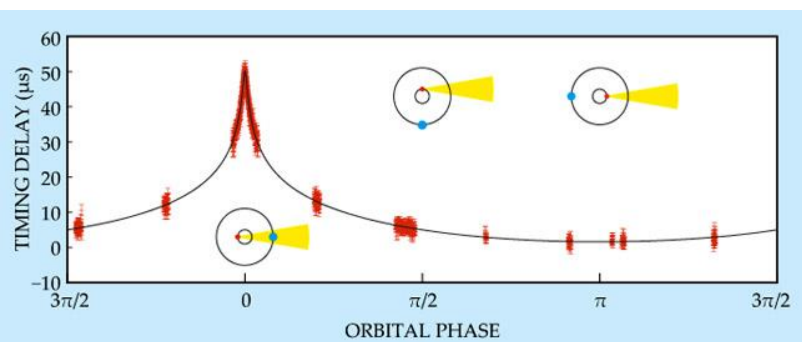


Demorest et al. (2010)

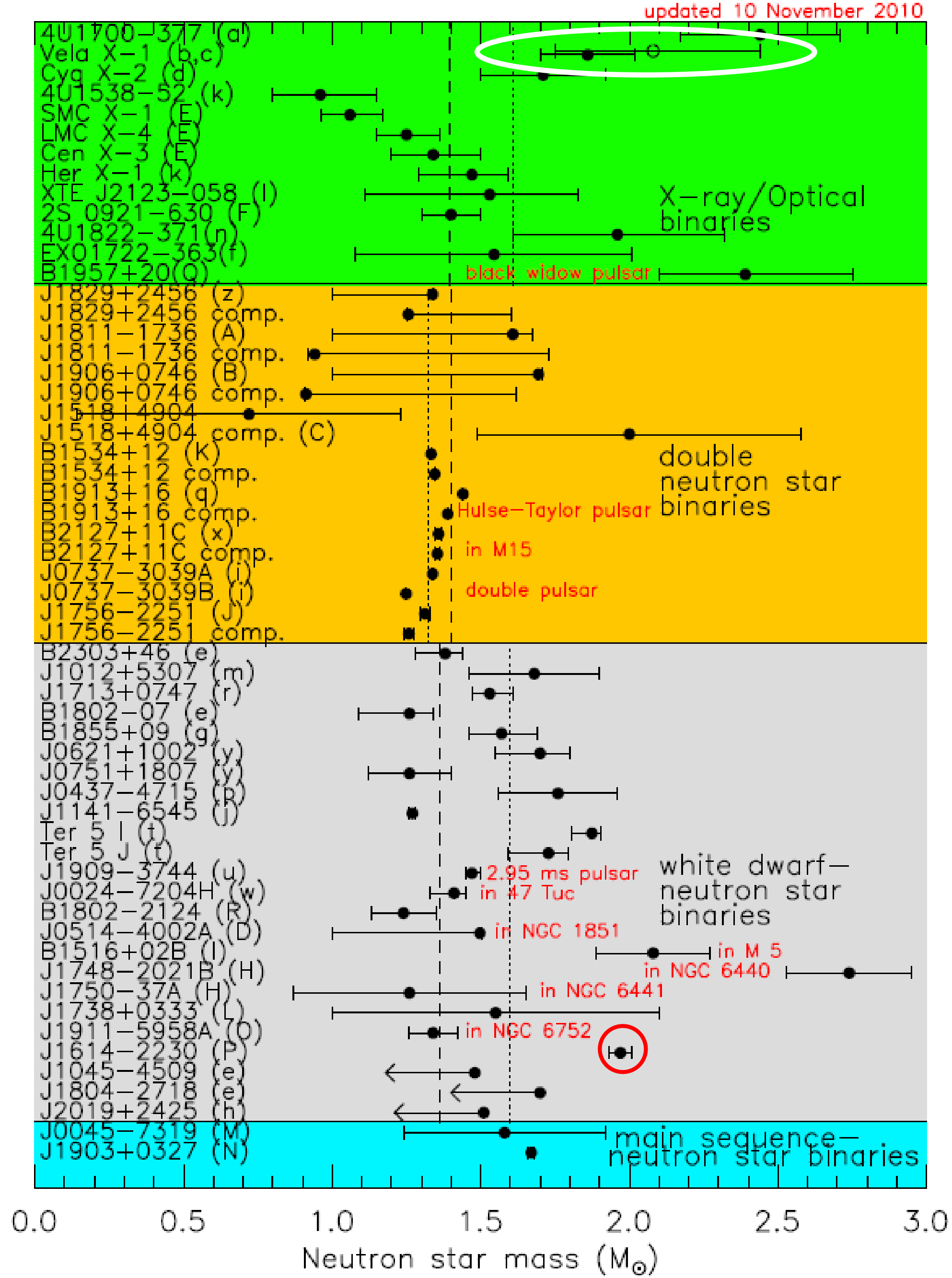


Lattimer & Prakash, arXiv:1012.3208.

# Mass-radius relation of light neutron stars

$$\eta = (K_0 L^2)^{1/3}$$

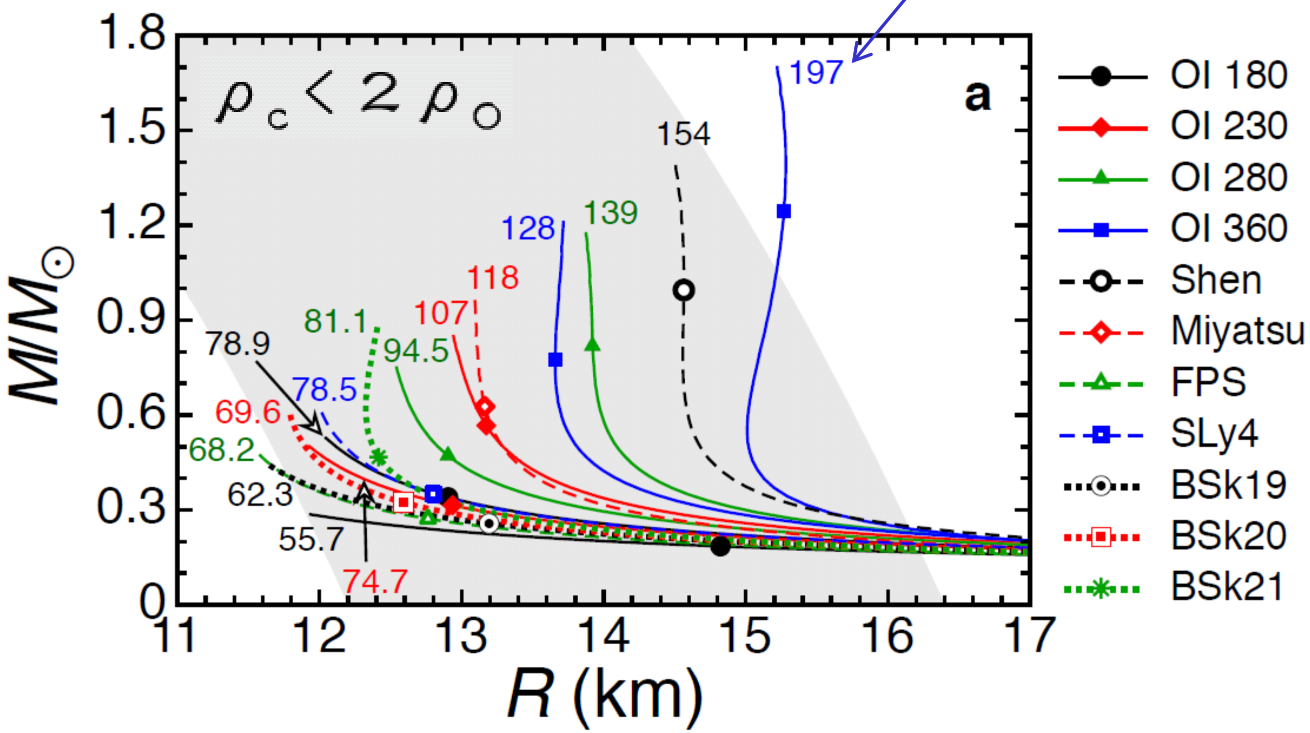


Sotani, Iida, Oyamatsu, & Ohnishi, arXiv:1401.0161.

In contrast,

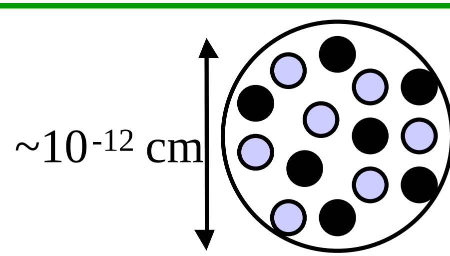


Atomic nucleus

$M \propto R^3$

# Mass and radius formulas for light neutron stars

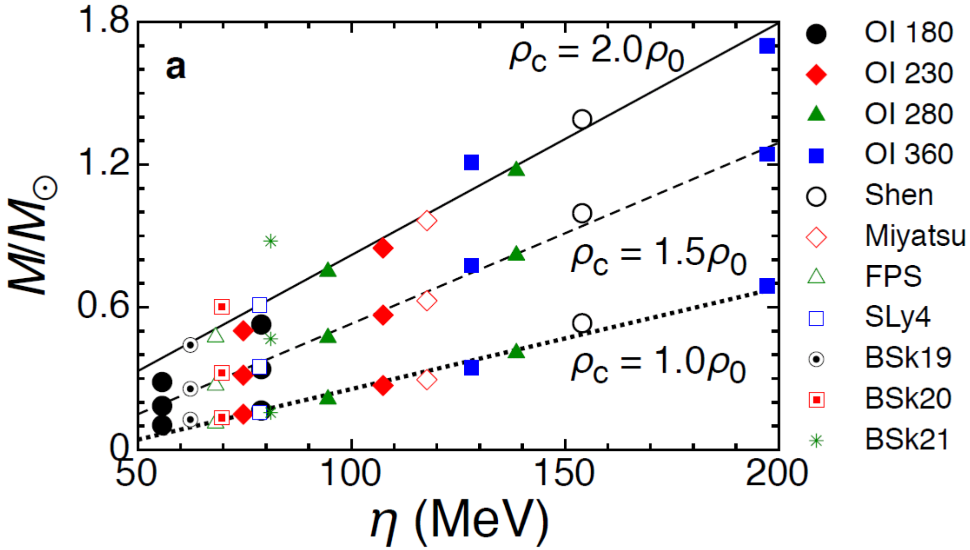


$$\frac{M}{M_\odot} = 0.371 - 0.820u_c + 0.279u_c^2 - (0.593 - 1.254u_c + 0.235u_c^2)\left(\frac{\eta}{100\,\mathrm{MeV}}\right)$$

$$\eta = (K_0 L^2)^{1/3}$$

$$u_c \equiv \rho_c/\rho_0$$

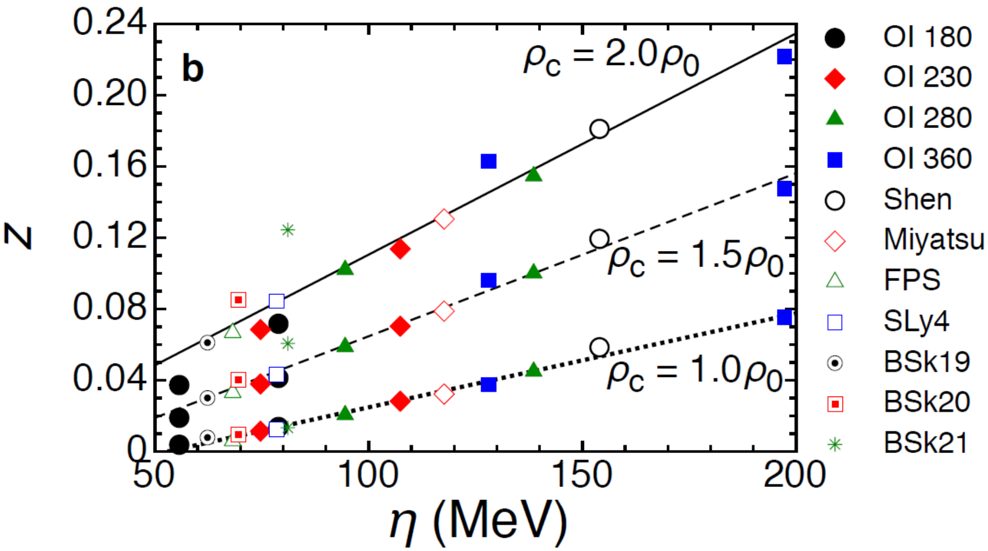


$$z = 0.00859 - 0.0619u_c + 0.0255u_c^2 - (0.0429 - 0.108u_c + 0.0120u_c^2)\left(\frac{\eta}{100\,\mathrm{MeV}}\right)$$

$$z = 1/\sqrt{1 - 2GM/Rc^2} - 1$$

Sotani, Iida, Oyamatsu, & Ohnishi, arXiv:1401.0161.

# X-ray burster 4U 1724-307

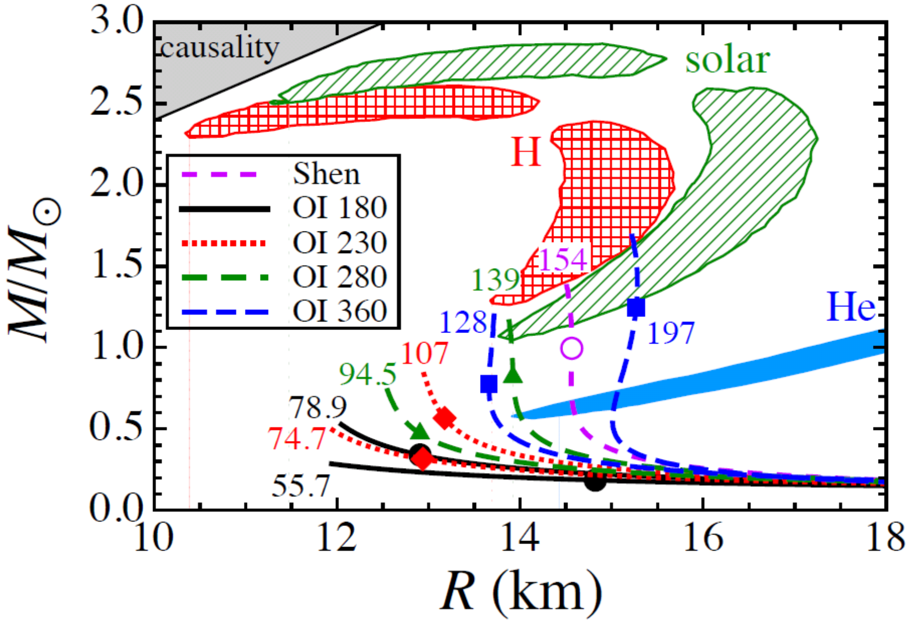


Large $\eta$ and hence $L$ suggested!

FIG. 3: (Color online) Allowed regions in the mass-radius relation obtained from the observation of the X-ray burster 4U 1724-307 by Suleimanov et al. [1], where they adopted three different atmosphere models, i.e., pure hydrogen (checkered region), pure helium (filled region), and the solar ratio of H/He with sub solar metal abundance $Z = 0.3Z_\odot$ (shaded region). On the other hand, the lines with marks denote the stellar models constructed from nine EOSs with different values of $\eta$ (attached numbers) for $\rho_c \leq 2.0\rho_0$, where each mark corresponds to the mass and radius of a star with $\rho_c = 1.5\rho_0$. Additionally, the upper left region is ruled out by the causality [38].

Sotani, Iida, & Oyamatsu, arXiv:1501.01698.

# Conclusion

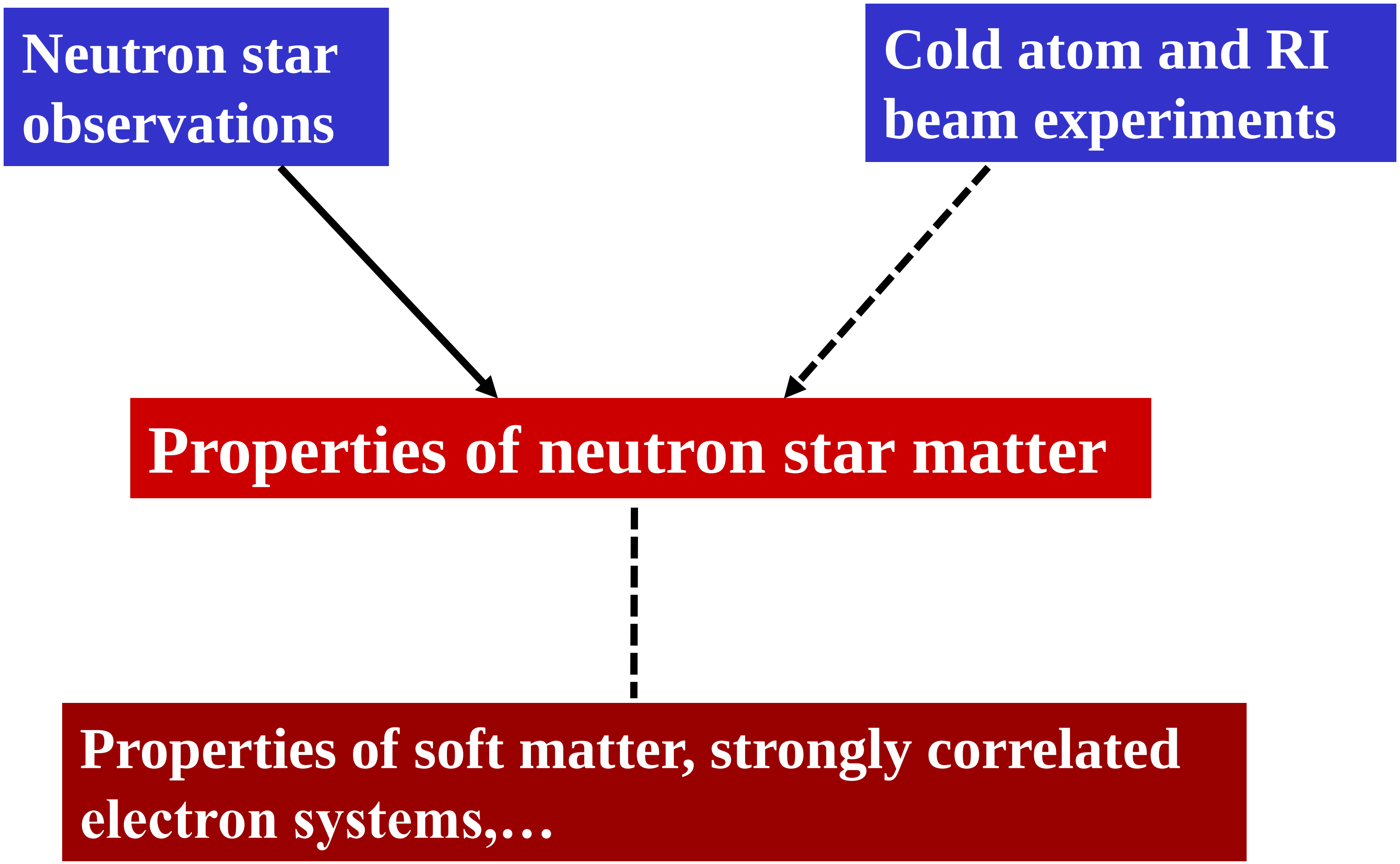
Neutron star observations
Cold atom and RI beam experiments
Properties of neutron star matter
Properties of soft matter, strongly correlated electron systems,…